AD_____

Award Number: W81XWH-12-2-0071

TITLE: Novel in vitro/ex vivo animal Modeling for Filovirus Aerosol Infection

PRINCIPAL INVESTIGATOR:
Ayesha Mahmood, Ph.D.

CONTRACTING ORGANIZATION: Sanofi Pasteur VaxDesign Corporation
Orlando, Florida, 32826

REPORT DATE: September 2014

TYPE OF REPORT: Annual

PREPARED FOR: U.S. Army Medical Research and Materiel Command
Fort Detrick, Maryland 21702-5012

REPORT DOCUMENTATION PAGE

Form Approved
OMB No. 0704-0188

1. REPORT DATE	**2. REPORT TYPE**	**3. DATES COVERED**
September 2014	Annual Report	15 Aug 2013 - 14 Aug 2014

4. TITLE AND SUBTITLE

Novel in vitro/ex vivo animal modeling for Filovirus aerosol infection

5a. CONTRACT NUMBER
W81XWH-12-2-0071

5b. GRANT NUMBER
W81XWH-12-2-0071

5c. PROGRAM ELEMENT NUMBER

6. AUTHOR(S)
Ayesha Mahmood, Ph.D.

email: Ayesha.Mahmood@sanofi.com

5d. PROJECT NUMBER

5e. TASK NUMBER

5f. WORK UNIT NUMBER

7. PERFORMING ORGANIZATION NAME(S) AND ADDRESS(ES)

Sanofi Pasteur VaxDesign Corporation

Orlando, Florida, 32826

8. PERFORMING ORGANIZATION REPORT

9. SPONSORING / MONITORING AGENCY NAME(S) AND ADDRESS(ES)

U.S. Army Medical Research and Materiel Command

Fort Detrick, MD 21702-5014

10. SPONSOR/MONITOR'S ACRONYM(S)

11. SPONSOR/MONITOR'S REPORT NUMBER(S)

12. DISTRIBUTION / AVAILABILITY STATEMENT
Approved for Public Release; Distribution Unlimited

13. SUPPLEMENTARY NOTES

14. ABSTRACT

The "Novel in *vitro / ex* vivo animal modeling for filovirus aerosol infection" program is a collaborative research effort between the USAMRIID Labs and Sanofi Pasteur VaxDesign to develop *in vitro* and *ex vivo* viral disease model systems composed of primary human and non-human primate cell lines, from species prone to filovirus infections. This work is relevant to the US Military due to the potential threat of biological bioterrorism in the military and civilian populations. To this end, Sanofi Pasteur VaxDesign is developing *in vitro* modular systems to dissect immunophysiological response to respiratory antigen of chemical and biological origin. This report summarizes the recent directions at the VaxDesign Sanofi Pasteur Campus related to quantitative methods to characterize barrier function, mode of antigen delivery, and related biological response to respiratory antigen. The *in vitro* mucosal tissue sensitivity was correlated with cellular composition, tissue confluence and chemical or biological agent entry pathways. The primary cell or cell line specific barrier function and related intrinsic tissue properties will be critical in the proposed *in vitro* VitroCell Cloud system. The mucosal tissue equivalent (MTE) module of the Modular Immune *In Vitro* Construct (MIMIC®) system were exposed to aerosolized phase antigen delivery including live attenuated and inactivated influenza vaccine. Similarly, the MTE product has been successfully infected with two strains of Ebola and Zaire by our USAMRIID collaborators. The methods relating to the cloud phase application of influenza antigen will be applied to filovirus infection model at USAMRIID labs.

15. SUBJECT TERMS: none listed

16. SECURITY CLASSIFICATION OF:			**17. LIMITATION OF ABSTRACT**	**18. NUMBER OF PAGES**	**19a. NAME OF RESPONSIBLE PERSON**
					USAMRMC
a. REPORT	**b. ABSTRACT**	**c. THIS PAGE**			**19b. TELEPHONE NUMBER** *(include area code)*
U	U	U	UL	46	

Table of Contents

1. INTRODUCTION

The "Novel in *vitro / ex* vivo animal modeling for filovirus aerosol infection" program is a collaborative research effort between the United States Army and Sanofi Pasteur VaxDesign (SPVD) to develop primary cell based tissue models for viral infections and therapeutic delivery. This work is relevant to the US Military due to the potential threat of bioterrorism in the military and civilian populations. This program explores the utility of *in vitro* human upper and lower airway tissue models for liquid and aerosolized mode of viral antigen or therapeutic delivery. The endpoint application for this model system is Filovirus related disease modeling with the use of primary human and non-human primate cell based models. Sanofi Pasteur VaxDesign is developing *in vitro* modular systems to dissect immunophysiological response to respiratory antigen of chemical and biological origin, appropriate for BioSafety Level 2 (BSL2) labs. The work builds on our previous systems, where primary human and non-human cells were used to design biologically relevant tissue models. The initial effort was concentrated on the design and characterization of the mucosal tissue equivalent module (MTE) based on cellular morphology, basic vesicle cycling, transcriptomic analysis of PRR and viral infection related genes, and innate immunological response respiratory antigen of bacterial (e. coli, staph aureus) and viral nature (live attenuated or inactivated influenza and inactivated filovirus strains). For the 2013-2014FY, the focus transitioned into aerosol and liquid phase mode of antigen delivery and similar biological readouts were re-visited. BSL2 grade influenza virus strains were selected for mucosal tissue equivalent (MTE) module exposure in the cloud or aerosolized phase alongside liquid phase application, to demonstrate the variation in the mode of antigen delivery and cellular response in the Influenza disease model. To this end, the focus of this report is on quantitative methods to characterize barrier function, and *in vitro* aerosol delivery and liquid phase delivery, where of live or inactivated influenza virus or vaccine studies demonstrate the biological response to select antigen. Each human and non-human primate model has its own intrinsic properties. We recognize the differences between *in vitro* and *in vivo* physiology and have decided to dissect the human respiratory models into upper and lower airway MTE modules. Our conclusions for the in vitro MTE modules are based on the contribution of cell types, tissue architecture, and the natural aerosolized mode of respiratory antigen delivery in our simplified high throughput system. Compared to the animal model gold standard, the in vitro infection and therapeutic screening platforms are more humane and cost effective. The overall objective of this program is directed towards Filovirus infection modeling. We have worked closely with USAMRIID labs to deliver the primary human lung MTE module product for the purpose of live infection with lethal strains of Ebola and Zaire virus at BSL4 USAMRIID. Preliminary live filovirus infection studies, reported by our USAMRIID collaborators, demonstrate the utility of the mucosal tissue equivalent (MTE) product of the MIMIC® system. The *in vitro* modeling criteria for current and future studies rely on biological knowns from the existing droplet and parenteral animal models, for filovirus challenge.

2. KEYWORDS:

Lung mucosal tissue equivalent, Humanized tissue models, Non-human primate tissue models, Upper and lower airway tissue models, Barrier function, Mass dependent permeability, Live and inactivated influenza antigen, Mode of antigen delivery, Aerosol cloud application, Mucosal Tissue Equivalent product shipment, Mucosal Tissue Equivalent infection

3. OVERALL PROJECT SUMMARY

The collaboration between USAMRIID and Sanofi Pasteur VaxDesign (SPVD) was proposed to develop *in vitro / ex vivo* respiratory tissue model using human and non-human primate cells to characterize cellular and localized biological function to aerosolized influenza and filovirus challenge and therapeutic delivery. The BioSafety Level-2 tissue engineering and influenza disease modeling work, at SPVD, was designed to develop a lung mucosal tissue equivalent (MTE) product for USAMRIID labs. The BioSafety Level-4 filovirus infection were performed at USAMRIID labs, using the MTE product. Completion of this work will facilitate the development of more efficient filovirus vaccines that induce a better immune response for protection against aerosol challenge.

Since much of human biology is still not well understood, our design philosophy of the lung MTE focuses on first principles, and is based on the elegance of simplicity and the conviction that increased complexity of design can be an impediment. A generalized fundamental core tissue module involves an extracellular matrix material sandwiched in between a confluent endothelium and a counter-positioned tissue-specific epithelium (e.g., nasal or alveolar). All MTE modules are constructed in a microtiter well format. We have achieved excellent success with fundamental tissue structure approximating alveolar function (i.e. APC function of type II epithelial cells, surfactant secretion, vesicle formation), and assessing various carcinogens, bacterial pathogens and immunosuppressants as discussed in previous reports.

In the 2012-2013FY primary cell and commercially available cell-line tissue models of human and non-human primate origin were selected based on the species susceptibility to filovirus infection. The lung epithelial cell lines including human (L-132, A549, and H292), non-human primate (4MBr-5), bat (TB 1 Lu), and mouse (LA4), were selected based on Ebola or Zaire infections at USAMRIID Labs. MTE models composed of primary human nasal and alveolar epithelium and endothelium were used as a comparative measure to the cell-line MTE model systems. Basic mucosal tissue equivalent (MTE) form and function were reported in the 2012-2013 Annual Report. The MTE designs were similar to our alveolar bilayer model shown in Firue A1. The Program Summary Table 1 summarizes the logical progression of the work based on program milestones and objectives.

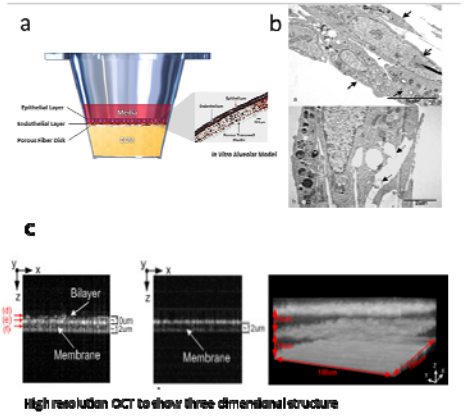

Figure 1A: Basic morphology of the alveolar mucosal tissue equivalent (MTE) a) cartoon representation of the hMTE set-up with image of actual immunohistochemical stained bilayer cross-section, b) transmission electron microscopy demonstration of differentiated alveolar Type II and Type I cells, c) Optical Coherence Tomography image of the tissue bilayer motif. *other MTE modules are designed similar to the alveolar hMTE

Based on the importance of mode of delivery on respiratory infections, we identified barrier function, mode of antigen delivery and cellular response to influenza antigen as the focus of FY 2013-2014 developmental work. We begin this Annual Report by presenting the logical experimental approach to a series of barrier function related studies. The tissue barrier

integrity, along with its ability to transport molecules processes directly affect local biological response. Herein, we describe a multifaceted approach to characterize the function of human cell line derived mucosal tissue constructs (MTE) in terms of transepithelial electrical resistance (TEER) of the mucosal tissue and molecular size based FITC-dextran transport. For the human models, the barrier TEER properties were also quantified with and without the addition of immune cells and biological mediators. This stepwise approach buildings system complexity and allows us to dissect quantifiable cellular functional contribution to the overall MTE immune response. These models also demonstrate barrier sensitivity to pro-inflammatory and immunosuppressive agents, including TNF-alpha and dexamethasone, respectively. Furthermore, the initial interrogation of FITC labeled dextran at various molecular weights was expanded into a larger study, where the mucosal transport of three different molecular weight molecules was quantified using a controlled approach to each human and non-human primate model system. Compared to the cell lines, the human primary cell models, especially the endothelium-containing motif, showed the highest degree of tissue integrity. The second section describes the preliminary experience with the *in vitro* aerosol delivery system, where graduated molecular weights of compounds were tested with select cloud droplet size settings. Single and multiple aerosol exposures of known respiratory irritants were applied along with multivalent Flumist® and Fluzone® vaccine formulations. The cellular response was qualified in terms of cytokine and chemokine response and antigen presenting cell surface marker expression. The third section of the report describes the nasal and alveolar mucosal tissue equivalent (MTE) model response to live influenza vaccine in liquid and aerosol phase. Table 1 shows the overall program overview. The 2013-2014 studies are highlighted in black for clarity.

The final sections of the report describe the live MTE product delivery and its utility as a filovirus infection model. A total of four shipments of MTE have been sent out to USAMRIID. The initial shipments were room temperature transport in tissue preservation media. We are in the process of transitioning into a portable incubator system in the next phase of the collaborative research effort. The USAMRIID scientists have confirmed the infection of alveolar MTE with Ebola and Zaire strains. The next steps include the addition of human peripheral blood monocytes as the target cells to the nasal and alveolar MTE modules.

Overall, our positive experimental findings indicate that both liquid and aerosolized mode of antigen delivery are the next phase of the program, and our systems are ready for live virus infection work and therapeutic testing. Having said, this, we still need to perform direct comparisons between aerosol delivery and liquid delivery of the antigen to assess if there are any benefits or consequences of aerosol delivery with wild-type virus strains. To date, our results indicate that aerosol delivery is less efficient in antigen delivery than liquid delivery, but we have no data to support the benefits of aerosol delivery. This is an on-going experimental study. The BioSafety Level-2 grade influenza strain infections will be characterized by antibody assisted labeling methods. In comparison, the Biosafety Level 4 filovirus strains are expected to infect and plaque more efficiently. We anticipate the addition of immune cells to the MTE product in the next phase of this program. The cellular viability and function, as it relates to live filovirus infection utility, will be an iterative collaborative effort between the SPVD and USAMRIID Labs.

			NHP cell line MTE				Primary human MTE				Human cell line MTE	
			4-MBr-5 Rhesus Monkey Bronchial	Tb1 Lu Bat Lung	Vero African Green Monkey Kidney	LA-4 Murine Lung Adenocarcinoma	Alveolar Epithelium	Nasal Epithelium	Alveolar Bilayer	Nasal Bilayer	A549 Lung Carcinoma	CRL1848 Lung Carcinoma
Airway Tissue	Tissue Integrity	Viability	☑	☑	☑	☑	☑	☑	☑	☑	☑	☑
		Confluence (live/dead staining)	☑	☑	☑	☑	☑	☑	☑	☑	☑	☑
		High resolution TEM	☒	☒	☒	☒	☑	☑	☑	☒	☑	☑
		FITC Dextran permeability (10KDA, 70KDa, 500KDa)	☑	☑	☑	☑	☑	☑	☑	☒	☑	☑
		Baseline transepithelial electrical resistance (TEER)	☑	☑	☑	☑	☑	☑	☑	☒	☑	☑
	Vesicle / membrane function	Membrane activity (epithelium dye uptake)	☑	☑	☑	☑	☑	☑	☑	☒	☑	☑
		Active vesicle cycling (time-lapse confocal imaging)	☑	☑	☑	☑	☑	☑	☑	☒	☑	☑
	Gene expression	PRR: TLR gene expression - TLR agonists	☒	☒	☒	☒	☑	☑	☑	☒	☑	☑
		PRR TLR expression- irradiated filovirus	☒	☒	☒	☒	☑	☑	☑	☒	☑	☑
		Cytosolic PRR RIG-I and NOD1- inactive filovirus	☒	☒	☒	☒	☑	☑	☑	☒	☑	☑
		Surfactant protein genes - inactive filovirus	☒	☒	☒	☒	☑	☑	☑	☒	☑	☑
		Mucin protein gene expression- inactive filovirus	☒	☒	☒	☒	☑	☑	☑	☒	☑	☑
	Secretory factors	Cytokine, chemokine response - TLR agonist-3,-4	☒	☒	☒	☒	☑	☑	☑	☒	☑	☑
	MTE module stability	MTE preliminary shelf leakage studies	☒	☒	☒	☒	☒	☒	☑	☒	☒	☒
	MTE Transfer	Product shipment (room temp or portable incubator)	☒	☒	☒	☒	☒	☑	☑	☒	☒	☒
	Aerosol Delivery	Molecular Weight Dependent aerosol dosimetery (10KDA, 70KDa, 500KDa FITC Dextran)	☒	☒	☒	☒	☒	☑	☑	☒	☒	☒
Airway Tissue Plus Immune Cells Biological Response	Tissue Integrity	TEER response - MTE plus monocytes	☒	☒	☒	☒	☑	☑	☑	☒	☑	☑
		TEER response – MTE plus monocyte with biological mediators	☒	☒	☒	☒	☑	☑	☑	☒	☑	☑
		TER response of monocyte plus MTE and TNF-alpha	☒	☒	☒	☒	☑	☑	☑	☒	☑	☑
	DC Phenotype	Bacterial antigen Inactive *Staphylococcus Aureus*	☒	☒	☒	☒	☑	☑	☑	☒	☑	☑
		Influenza vaccine (FluMist®, Fluzone®)	☒	☒	☒	☒	☑	☑	☑	☑	☑	☑
	Secretory factor	Cytokine and chemokine response Bacterial antigen-inactive *Staphylococcus Aureus*	☒	☒	☒	☒	☑	☑	☑	☒	☑	☑
		Cytokine and chemokine response Influenza vaccine-FluMist®, Fluzone®	☒	☒	☒	☒	☑	☑	☑	☑	☑	☑
	Aerosol Delivery	Dingle and double antigen dosimetery (Flumist®, Fluzone®, Staph Aureus BP, E Coli BP, histamine	☒	☒	☒	☒	☑	☑	☑	☒	☒	☒

Table 1: Program Summary Table for the "Novel *in vitro*/ex vivo animal modeling for Filovirus aerosol infection" program. The black highlighted sections show the studies in 2013-2014. There was an overlap with 2012-2013FY with the added aerosol mode of delivery. The green check mark denotes executed studies.

PART 1: Baseline barrier function of human and non-human primate tissue models

Introduction and Experimental Logic

The overall objective of this program is related to the development of biologically relevant tissue models to help better understand viral disease pathogenesis and therapeutic delivery to respiratory mucosa. This work focuses on the *in vitro* tissue model systems and draws its design inspiration from examining the fundamentals required from *in vivo* biology. The epithelial and endothelial tissue at the mucosal barrier interfaces are directly involved in transport processes to and from the host and its environment. These processes can be observed both by direct transfer of substances and/or by the resultant local tissue response. In general, the cellular functional response is identified by chemical, biological, and energetic signature physiology. Herein, we report the baseline *in vitro* tissue barrier properties in terms of transepithelial electrical resistance (TEER) measurement over time, along with mass transfer of controlled molecular weight of fluorescently labeled dextran solutions. These *in vitro* models were designed to directly compare tissue integrity of primary cell and cell lines, which are of interest in highly pathogenic influenza and filovirus infections. To elaborate on the barrier function of our *in vitro* models, pro-inflammatory cytokine TNF-alpha and immunosuppressive agent dexamethasone, were introduced to the tissue models. The MTE models with and without the addition of peripheral blood mononuclear cells (PBMC) served as controls for each human MTE model system. Methods for *in vitro* antigen delivery to and from mucosal interfaces are highly relevant to understanding infection, disease pathogenesis and therapeutic delivery.

The mucosal interfaces serve as primary line of defense for antigen entry, from the environment to the local tissue leading to systemic circulation. Specifically, the epithelial tissue tight junctions serve as entry gates paracellular and intracellular pathways. The mucosal barrier physiological response is of direct relevance to the disease pathogenesis. The local peripheral vasculature also serves as a barrier at these interfaces. Here, the mucosal-vasculature interface neutrophil recruitment process serves as a protective measure to regulate foreign body recognition and entry via membrane interaction, protein synthesis, reactive oxygen species, enzymatic pathways, and cytokine response. However, this direct access from the local mucosa to systemic circulation also results in dysregulated processes including tissue and organ injury, during pathogenesis. Thus, the biology of disease pathogenesis is dependent on the tissue barrier function (Fischbarg, 2010; Kreijtz, 2011; Armstrong, 2012; Sedgwick, 2002; Grommes 2010). Reproducing mucosal entry pathways (*in vitro*) is critical to developing biologically relevant *in vitro* biomimetic models of viral infection. Our simplified approach to address tissue barrier response of human and non-human primate MTE started with the characterization of electrical resistance and controlled molecular mass transfer studies.

A number of approaches were applied to quantify mucosal tissue physiology. The transepithelial resistance (TEER) measure is a basic method to determine the level of tissue integrity and energetic signature by applying a mild alternating current to a cell layer. This quantitative method is related to paracellular and subcellular activity responsible for tissue permeation properties. The resistance measure in the *in vitro* system is dependent on the

tissue layer, culture medium, type of transwell plastic material, and the positioning and quality of the electrode. To this end, each measurement needs to be normalized and overall trends are relative to the experimental conditions. The TEER quantitative measure was used in conjunction with other quantitative methods, as it is not an accurate stand-alone measure of barrier function (Benson, 2013). Thus, we have also identified the FITC-dextran permeability assay as the alternative method. This assay is clinically used to identify and diagnose lung injury (Briot, 2009; Bayat, 2008). Our preliminary results (2012-2013 Annual Report) showed a relationship between the level of cellular extravasation and tissue integrity, as identified by FITC dextran permeation. The degree of gap junction cell-cell, cell-substrate contact was measured by the addition of 10KDa, 70KDa and 500KDa FITC-dextran molecules, to better understand mass transfer as it relates to mucosal barrier permeability.

This section addresses the tissue integrity function of nine human and non-human primate tissue models via both TEER and mass dependent FITC dextran permeation studies. The *in vitro* mucosal tissue equivalent (MTE) modules were composed of primary human nasal and alveolar epithelial / endothelial cells, along with A549 and CRL-848 cell lines. The NHP models were composed of 4MBr-5 (Rhesus monkey), Tb1Lu (bat), LA-4 (murine), and Vero (African green monkey) cell lines. The tissue characterization of the NHP models was reported in the 2012-2013 Annual report. Besides baseline TEER function, here we also tested the addition of pro-inflammatory TNF-alpha and immunosuppressive dexamethasone in the in the human model systems. The addition of chemical stimulants or suppressants to the cell layer can alter the overall epithelial resistance energetics of baseline tissue response. The FITC dextran permeability was also re-visited with larger replicate set-ups and fine-tuned experimental conditions to confirm the TEER experimental findings that define intrinsic properties of the nine MTE tissue models.

Experimental approach to tissue confluence or "Leakiness" via transepithelial electrical resistance and molecular weight dependent permeability studies

Cell culture

Primary human nasal and alveolar cells (Promocell), A549 (ATCC), and CRL-1848 (ATCC) were expanded in T-175 flasks in airway cell media. Passage 3-4 cells were used for tissue model studies. The primary tissue models were prepared by seeding 50,000 cells on a transwell in 10% serum containing 1:1 (v/v) Media199 and DMEM with 1% penicillin-streptomycin (sigma). For the NHP models, 4MBr-5 Rhesus monkey cell line, Tb1Lu Bat cell line, LA-4 murine cell line, and Vero African green monkey cell line were purchased from ATCC and expanded up to passage eight in the ATCC recommended media formulations. For the experiments, the cultured cell lines were grown in 30% serum containing HAM's FK-12 base media. 4-MBr5 cell line was cultured without EGF after the initial expansion up to passage eight. Media was exchanged every 48hr until confluent. For the cell lines, cell seeding density was 35,000 cells/per well. Tissue layer formation was observed between 3-4 days for the cell lines and 5-7 days for the primary cells. The experiments were staggered to take into account the growth rates so the stimulations were done on differentiated tissue constructs. A dedicated set of plates was

assigned for each model system to limit plastic ware variation for the TEER and FITC dextran quantification studies.

Transepithelial Electrical Resistance (TEER)

Electrical resistance was measured using the STX2 Endohm-6 system from World Precision Instruments. Confluent tissue constructs were placed in the central chamber of Endohm-6, with a fixed electrode at the bottom along with a variable height electrode at the top of the tissue layer. The height of the top electrode was kept constant for all the experiments; see Figure 1. All MTE modules were incubated at 37^{o}C and the TEER readings were taken within five minutes of room temperature exposure. A total of ten replicate conditions were sacrificed at three different time points for the nine human and non-human primate models consisting of primary alveolar epithelium, nasal epithelium, alveolar bilayer (epithelium and endothelium), along with A549 (human lung), CRL-1848 (human embryonic), LA-4, Tb-1Lu, 4MBr5, and Vero cell lines. The mucosal tissue TEER value was measured at 24, 48, and 72 hours after complete confluence of the tissue, as described in our earlier reports. The MTE tissue modules composed of A549 and CRL-1848 cell lines were compared against primary human alveolar and nasal epithelium, along with the alveolar bilayer models (epithelium and endothelium). For the NHP models, 4MBr-5 Rhesus monkey cell line, Tb1Lu Bat cell line, LA-4 murine cell line, and Vero African green monkey cell line were tested. The baseline resistance readout was recorded by using transwell buckets without cells in culture media for characterizing the baseline MTE stability profiles. Each of the ten conditions had a corresponding medial control transwell. The normalized TEER values were determined by subtracting the blank transwell readout from the confluent tissue containing chambers.

TEER sensitivity to PBMC addition along with pro-inflammatory and immunosuppressive agents

The experimental set-ups for this study were similar to the TEER section (above) with the addition of peripheral blood mononuclear cells (PBMC) to the MTE modules. Each condition was tested with twelve replicates in multiple plate set-ups, to characterize well-to-well variation. Twelve no treatment conditions were tested in the same base media to normalize the readouts. The tissue constructs were washed with serum-free base media prior to the addition of one million PBMC for ninety minutes. This step replicates the initial peripheral blood mononuclear adhesion step *in vivo* and builds immunophysiological complexity in the system. The apical chamber was washed with base media (x2) prior to the addition of TNF-alpha or dexamethasone, followed by TEER readouts. TNF-alpha or dexamethasone was added at a concentration of 10ng/ml. The TEER readings were recorded after two hour MTE incubation at 37^{o}C, 5%CO_2. The normalized TEER is shown in terms of Ohms in Figure 2.

FITC-dextran transport

FITC-dextran permeability studies were designed as a secondary measure to quantify tissue integrity. The tissue models were prepared as described above. For permeability studies,

human and non-human primate tissue cell layers were washed with M199 (x2). This was followed by 700ul of M199 addition to the receiver bucket and the apical side was exposed to air interface for 2hr. Serial dilutions for FITC-dextran (MW 10KDa, 70KDa, 500KDa; Sigma-Aldrich) stock solution were made and added to the apical side of the construct. Eight tissue constructs were sacrificed per time point (30, 180, 360min). The apical and basal media was collected and read at 485nm/535nm wavelength. The data was reported in terms of concentration (mg/ml) based on the standard curve for each dextran molecule, Figure 4a. The data was also converted into a static chamber permeability coefficient; Figure 4b .

Part I: Results and Discussion

Each MTE model system produced cell type specific electrical resistance signature reading; Figure 2. This electrical resistance measure serves as a baseline MTE barrier stability on the day of infection or antigen introduction. On its own, the baseline TEER is not directly related to tissue permeability of antigen, as the intuitive higher cell line resistance value for TEER readout is indicative of the cellular over-growth or "layering effect". Thus, a stable TEER reading is reflective cellular growth plateau or contact inhibition leading to a stable tissue layer. The epithelial resistance readouts show the highest level of stable confluence in the primary alveolar tissue model, when directly compared against the human cell line containing MTE modules; Figure 2. This includes both the alveolar and nasal epithelium alone and the alveolar epithelium plus endothelium containing MTE modules. The higher level of electrical resistance in the alveolar bilayer model, over the alveolar epithelium alone, was attributed to the additional endothelial layer, since the epithelium alone generated a lower electrical resistance profile. The additional endothelial layer improved the electrical resistance in the system. The primary nasal MTE module showed a decline in electrical resistance after the initial 24 hours. We hypothesize that this is a result of tissue differentiation into the intrinsically leaky interface. Altogether three sets of studies with 6, 10 and 12 replicates conditions show this effect. The human A549 and CRL-1848 showed relatively wider range of TEER readouts. This suggests a less stable tissue barrier function or reduced cell-cell tight junction contact by the cell line layers. Compared to primary human MTE models, there was more well-to-well variation in the human and non-human primate cell line models, with the exception of Vero cell line. The baseline TEER readout is not directly related to confluence, and can only be used as a stability measure of cellular growth. The cell line over overgrowth and irregular cell arrangement has been previously reported for the MTE models; see the tissue integrity related sections in program summary Table 2. The results for the MTE models suggest that each cell type has its own intrinsic characteristic for electrical resistance and the primary cells show higher cellular stability over the three-day measurement. The following section re-visits the validity transepithelial resistance (TEER) method with the addition of immunopotentiators and quantifies the barrier function in terms of FITC-dextran permeability.

The mucosal site is an antigen recognition interface that communicates with the local tissue. The addition of chemical stimulants or suppressants to the mucosal layer can alter the overall epithelial resistance energetics of the baseline response and replicates the additive effect of chemical and biological antigen. With the addition of immunopotentiators, the electrical

resistance value gives us insight into the natural extravasation processes of preliminary monocytes adhesion step on the mucosal tissue layer(s). This immunophysiological response can be measured by comparing the cell-cell and cell-substrate interaction by quantitative energetic methods, ranging from simple electrical resistance, and impedance to more complex atomic force evaluation of the system. Furthermore, the energetic response is sensitive to the addition of immunopotentiators. For example, the addition of pro-inflammatory cytokines has been shown to reduce the transepithelial electrical resistance and increase in tissue deformation to permit the migration of monocytes and other chemicals to the inflammation site (Kataoka, 2002; Ge, 2009). Our preliminary step, to build MTE complexity, was the addition of immune cells to the MTE modules. Figure 3 shows direct comparison of TEER differentials due to PBMC addition to MTE modules. Overall, the immune cell addition resulted in an increase in electrical resistance in all the human primary cell and cell line models. We hypothesize that this response is similar to the higher TEER values of the bare cell line MTE modules and likely due to the cellular stacking due to adhesion, on the MTE. Thus, the TEER measurements of MTE modules with immune cells serve as a baseline tissue readout to the immunopotentiators interaction study.

Of the five MTE modules, the alveolar bilayer model showed significant electrical resistance sensitivity to both pro-inflammatory TNF-alpha and immunosuppressive dexamethasone. In general, dexamethasone increased electrical resistance function of the primary cell MTE models. Whereas, no significant TEER response to dexamethasone for the A549 and CRL-1848 cell lines. Pro-inflammatory cytokine TNF-alpha reduced the TEER readout for the primary cell models. These findings are in agreement with controlled studies on processes relating the effect of pro-inflammatory or suppressive agents on immunophysiological function (Kataoka, 2002; Ge, 2009). We hypothesize that the endothelial layer in the bilayer model improves the cellular response. Similar to the alveolar model, A549 cell line also showed a significant decline in electrical resistance to TNF-alpha. Whereas, the CRL-1848 cell line was least responsive. The electrical resistance results imply a cell type dependent baseline response that is specific to primary cells and cell lines.

Permeability studies and implications on innate immune response

The transepithelial electrical resistance and FITC-dextran studies demonstrate quantitative means to measure barrier function of our *in vitro* biomimetic model systems; Figure 4a,b. In general, increased electrical resistance readout is associated with more open cell-cell contact due to less tight binding junctions. These open motifs permit passive transport (permeability) of plasma and associated cells and soluble agents. The *in vitro* electrical resistance measurements are dependent of electrode sensitivity and experimental design and require sample normalization. Furthermore, the use of multi-layer cellular model systems introduces electrical resistance increase that is not directly related to tissue confluence or permeability and only serves as a cell type specific baseline tissue stability measure. The use of immunopotentiators for the TEER studies demonstrates cellular response to selective antigen. A complementary FITC-dextran permeation study was designed to further quantify tissue barrier function through transfer of inert dextran molecules. Based on the two quantitative measures, we conclude that

the primary human bilayer model is a stable tissue motif with sensitivity to pre-inflammatory mediator (TNF-alpha) and immunosuppressive (dexamethasone). The bilayer model also has the least level of FITC-dextran permeability. Overall, the cell line models showed a lack of tissue electrical resistance stability and the highest degree of molecular weight independent, non-selective FITC dextran permeation.

On its own, the baseline electrical resistance of the various tissue models is not a conclusive measure of the level of tissue confluence or permeability. However, the addition of immunopotentiators with and without the addition of peripheral blood mononuclear cells (PBMC) is indicative of mediator response to tissue physiological function. The addition of PBMC increased electrical resistance in all the tissue models. The resulting TEER differential is due to the initiation adhesion step of monocyte migratory processes through increase in cellular tight junction interactions between the airway tissue and the monocytes; this serves as a baseline for the addition of immunopotentiators and does not directly serve as a comparative measure of barrier function of the MTE models. The initial increase in electrical resistance after monocyte addition is attributed to the monocyte adhesion response; this is similar to the "layering effect" by the cell lines baseline TEER readouts (Figure 3). We anticipate the electrical resistance to decrease with the migration of the monocytes after the adhesion step.

The stimulant (TNF-alpha) / suppressant (Dexamethasone) related study supports the alveolar bilayer function in terms of selective sensitivity to these classic immunopotentiators and related leukocyte recruitment to the inflamed tissue. TNF-alpha is a known hyperpermeability cytokine, which reduces electrical resistance in the local tissue and increases antigen and cellular permeability. The TNF-alpha and dexamethasone response in the *in vitro* model system is in agreement with barrier function related electrical resistance and permeability studies (Kumar, 2009; Kataoka, 2002; Ge, 2009). The dampened response of alveolar epithelium and the nasal epithelial models demonstrates the relevance of endothelium in the *in vitro* alveolar bilayer model system in the presense of a pro-inflammatory agent like TNF-alpha. This bilayer model is most biologically relevant since the addition of endothelium to the mucosal epithelium mimics the interaction between the local tissue and the local vascular network. The A549 and CRL-1848 cell line function was not comparable to the physiological function of primary cell lines.

The non-human primate cell lines were not comparable to the alveolar bilayer model in the TEER and FITC-dextran permeability measures. There was also more well-to-well, plate-to-plate variation in these model systems; this phenomenon is due lack of cell junction molecule interactions and overall confluence of the tissue layer. Furthermore, we were not able to test monocyte related studies for the NHP model systems due to lack of leukocyte availability. However, the human and non-human primate cell line trends were similar to cellular junctions and/or a non-confluent tissue layers observed in our previous findings (2012-2013 Annual Report). Based on this, the molecular weight independent FITC dextran results are in agreement with the non-stable baseline epithelial resistance measurements demonstrate similar types of response for all cell line model systems. The addition of immunopotentiators resulted in unexpected little to no functional response by CRL-1848. Compared to the primary

cell models, the A549 cell line showed a different base line and differential response to TNF-alpha. Thus, the use of cell lines may always need to be compared against and relative to the *in vitro* or *in vivo* primary cell response.

FITC-dextran transport

FITC-dextran permeability interrogation was re-visited in larger replicates, as a means to support the barrier function findings. Three different molecular weights (10KDa, 70KDa, 500KDa) of FITC-dextran were studied to correlated molecular size with mass transfer characteristics. The dextran permeability results are shown in Figure 4 (a, b) and 5 for human and non-human primate model system, respectively. The data for the human models was converted into endpoint specific permeability constants in a equilibrating MTE. Whereas, the degree of quantified FITC-dextran mass transfer in the animal models is illustrated by the green line graph. The blue line graph represents the apical supernatant quantification of dextran. A dedicated plate set was used for each tissue model permeability study. As a result, this data set is more consistent with our hypothesis relating to antigen size dependent permeability through primary cell and cell line containing tissue interfaces.

The increased tissue permeability, leukocyte recruitment, and plasma leakage is related to intrinsic cellular tight junction proteins and the junction-intracellular enzymatic and energetic pathways. These processes are evoked by hyper-permeability mediators like histamine, thrombin, leukotrienes, and cytokines. These biological mediators directly interact with the cell surface molecules and tight junction proteins. Thus, the primary cells and cell lines are expected to have differences in cell-cell and cell-substrate interactions (Kumar 2009) based intrinsic differences in the cellular make-up and the tissue architecture. To simplify the physiological response, a basic permeability study was designed to directly compare nine MTE modules. Fluorescently labeled dextran was selected due to its inert nature and commercial availability of various molecular weights of the molecule. Samples were introduced to relatively equivalent concentrations of FITC dextran in each model system. The amount of material on the apical and basal side of the tissue layer served as a direct measure of tissue permeation; see Figure 4, 5. For the primary human alveolar bilayer MTE, the results show minimal dextran permeability. This response was anticipated since the endothelial layer has more tight junction contact compared to the epithelial tissue. It is to be noted that there is a mild increase in the basal level of dextran by the 360min time interval. The alveolar epithelium alone showed a lack of permeability with an increase in dextran molecular weight. At any given time interval, the percent transfer or quantified amount 10KDa FITC-dextran in the basal compartment was higher than the amount of FITC-dextran in the 70KDa or 500KDa experiments. The upper and lower airway mucosa is made-up of difference cell types with variances in intracellular and paracellular properties. This may direct implications to the application of airway allergens and histamine response via known airway entry pathways (Kumar 2009). The cell line models of human and non-human primate origin showed a higher level of dextran permeability with negligible molecular weight or antigen size selectivity. The TEER results and the FITC dextran study show distinct differences in primary cells and cell line barrier function. Part I results summary table R1 demonstrates the graduated TEER response readout of the various MTE

models. Whereas, Table R2 shows the tissue permeability measure in terms of quantified basal FITC-dextran. For the NHP MTE the Vero cells show the highest degree of selectivity to FITC-Dextran. However, the Vero cells are not of lung origin and cannot be used as a representative lung model system. The alveolar bilayer showed a higher degree of selectivity for the human MTE modules. Results summary table R3 demonstrates the biological sensitivity to immune mediators in the lung humanized MTE. The alveolar bilayer and A549 cell line performed the best in terms of selective response to pro-inflammatory TNF-alpha treatment. The relative response to immunosuppressive dexamethasone was significantly higher in the alveolar bilayer model. We have demonstrated the strengths and weakness of barrier function in both human and NHP model system. The rest of the sections are dedicated to cellular response as it related to mode of antigen delivery in the human MTE models. We selected the human models based on the ease of access to immune cell source for the work.

	NHP cell line MTE				Primary human MTE			Human cell line MTE	
	4-MBr-5 Rhesus Monkey Bronchial	Tb1 Lu Bat Lung	Vero African Green Monkey Kidney	LA-4 Murine Lung Adenocarcinoma	Alveolar Epithelium	Nasal Epithelium	Alveolar Bilayer	A549 Lung Carcinoma	CRL1848 Lung Carcinoma
Baseline transepithelial electrical resistance (TEER)	+++	+	++	+++	+	+	++	++	+++

Table R1: Basic transepithelial response from the human and non-human primate MTE models.
(+), (++), and (+++) are arbitrary assignments that reflect the degree of signal. A "+++" signal is indicative of cellular stacking and overgrowth.

	NHP cell line MTE				Primary human MTE			Human cell line MTE	
	4-MBr-5 Rhesus Monkey Bronchial	Tb1 Lu Bat Lung	Vero African Green Monkey Kidney	LA-4 Murine Lung Adenocarcinoma	Alveolar Epithelium	Nasal Epithelium	Alveolar Bilayer	A549 Lung Carcinoma	CRL1848 Lung Carcinoma
FITC-Dex permeability 10KDa (basal MTE) relative to time 0	(+) P<0.0001	(+) P<0.0001	(+) P<0.0001	(+) P<0.0001	(+) P<0.0001	(+) P<0.0001	(+) P<0.0001	(+) P<0.0001	(+) P<0.0001
FITC-Dex permeability 70KDa (basal MTE) relative to time 0	(+) P<0.0001	(+) P<0.0001	(-) P<0.0001	(+) P<0.0001	(+) P<0.0001	(+) P<0.0001	(+) P<0.0001	(+) P<0.0001	(+) P<0.0001
FITC-Dex permeability 500KDa (basal MTE) relative to time 0	(+) P<0.0001	(+) P<0.0001	(-) P<0.0001	(+) P<0.0001	(+) P<0.0091	(-) ns	(-) ns	(+) P<0.0001	(+) P<0.0001

Table R2: FITC-Dextran permeability to the basal MTE.
(+) assignment reflects permeability through the MTE, (-) assignment reflects the lack of permeability.

	Primary human MTE			Human cell line MTE	
	Alveolar Epithelium	Nasal Epithelium	Alveolar Bilayer	A549 Lung Carcinoma	CRL1848 Lung Carcinoma
TEER response of MTE + PBMC relative to MTE	(+) P<0.0001	(+) P<0.0001	(+) P<0.0001	(+) P<0.0001	(+) P<0.0001
TEER response to immune mediators – MTE + PBMC + dexamethasone relative to MTE plus PBMC	(-) ns	(-) ns	(+) P<0.0001	(+) P<0.0163	ns
TEER response to immune mediators – MTE + PBMC + TNF-alpha relative to MTE plus PBMC	(+) P<0.0001	(-) ns	(+) P<0.0050	(+) P<0.0001	ns

Table R3: Human MTE response to immune modulators (dexamethasone, TNF-alpha)
(+) assignment reflects the expected response above the control condition, (-) assignment reflects the lack of expected response when compared against the control condition.

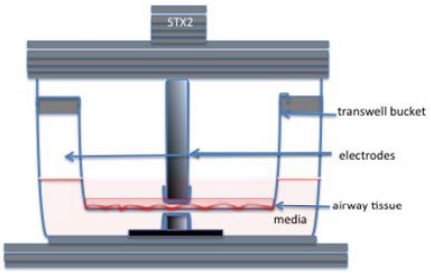

Figure 1: Schematic diagram of transepithelial electrical voltammeter

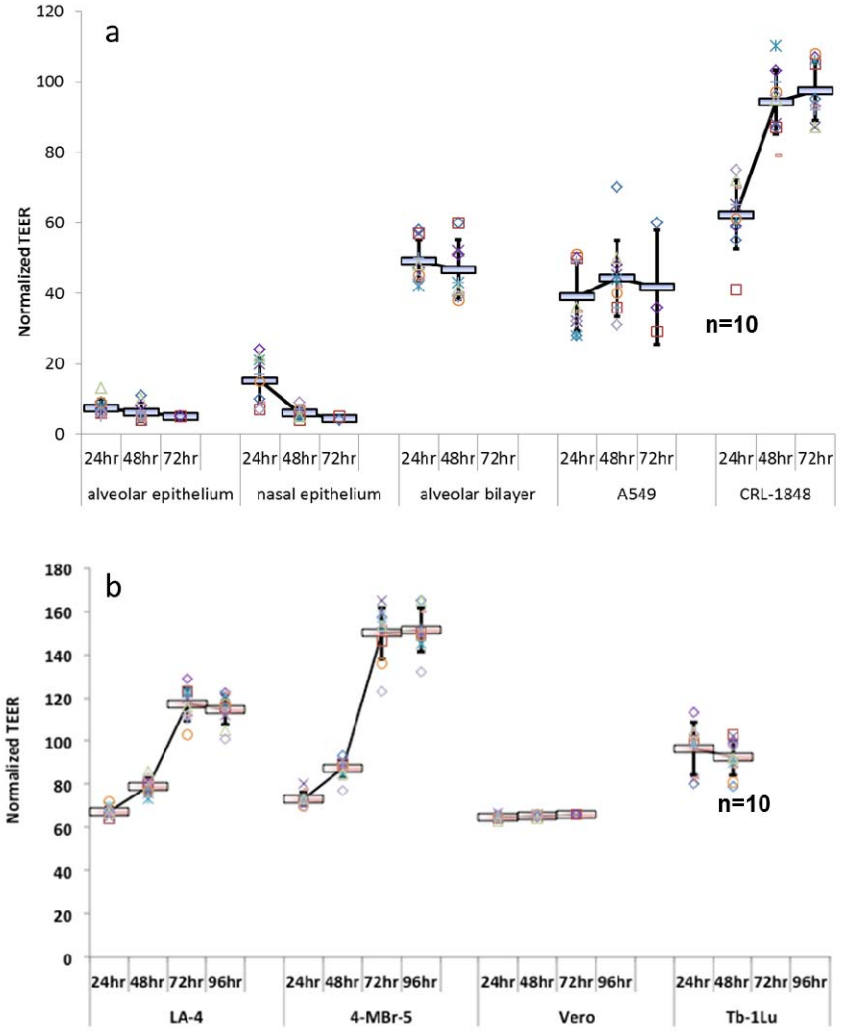

Figure 2: Kinetic transepithelial electrical measurement (ohms) of a) human mucosal tissue models, b) non-human primate tissue models

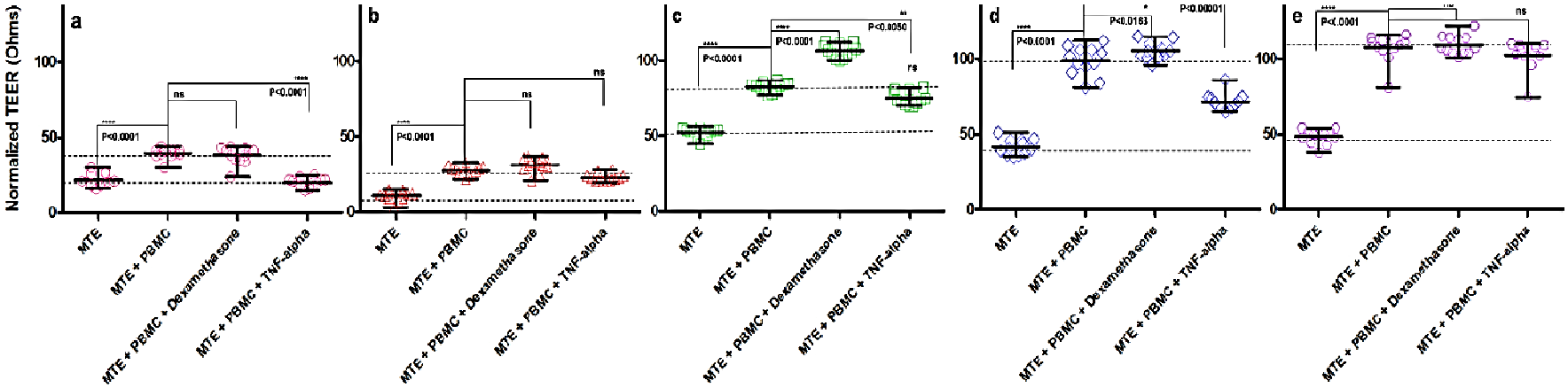

Figure 3: The effect of immunopotentiators on the tissue electrical resistance with the addition of peripheral blood mononuclear cells to the MTE composed of differentiated a) alveolar epithelium, b) nasal epithelium, c) alveolar bilayer, d) A549 cell line, e) CRL-1848 cell line. Each condition was tested in multiple plate set-ups (n=12) and Tukey's multiple comparison test was used with 2-way ANOVA. The results show statistically significant physiological response to chemical mediator treatment by the alveolar bilayer MTE. The alveolar epithelium and A549 cell line response to TNF-alpha was physiologically relevant and anticipated. However, the little or no response to dexamethasone by the alveolar epithelium, nasal epithelium and CRL-1848 shows the importance of *in vitro* cell type selection to mimic biological response.

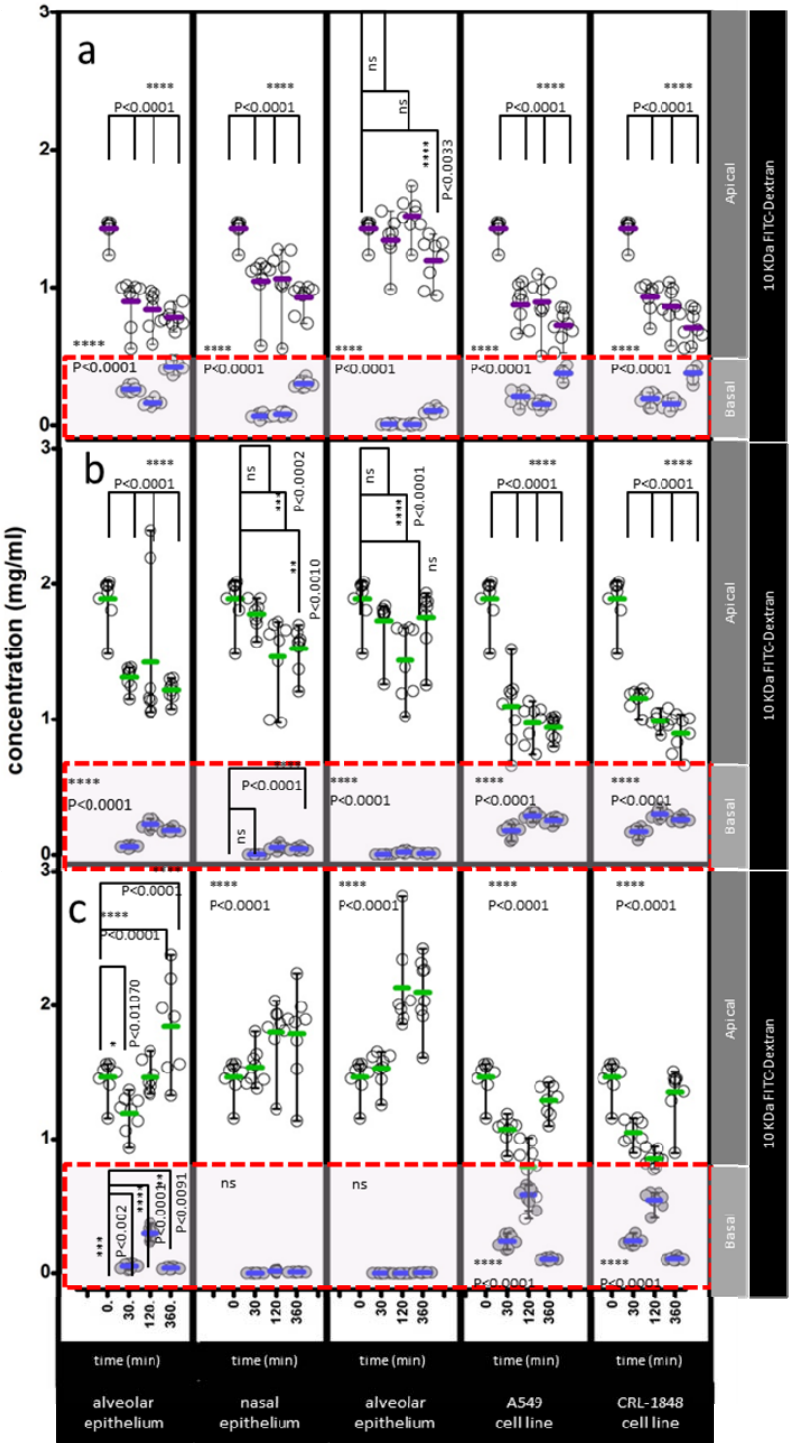

Figure 4: Direct comparison of real-time FITC-Dextran transport through the MTE modules. The FITC-Dextran a) 10KDa, b) 70KDa, c) 500KDa solution were applied to the apical side of the MTE. Eight modules were sacrificed at each time interval. Dunnett's multiple comparison 2way ANOVA was done to compare the kinetic differentials in the apical and basal observed concentrations.

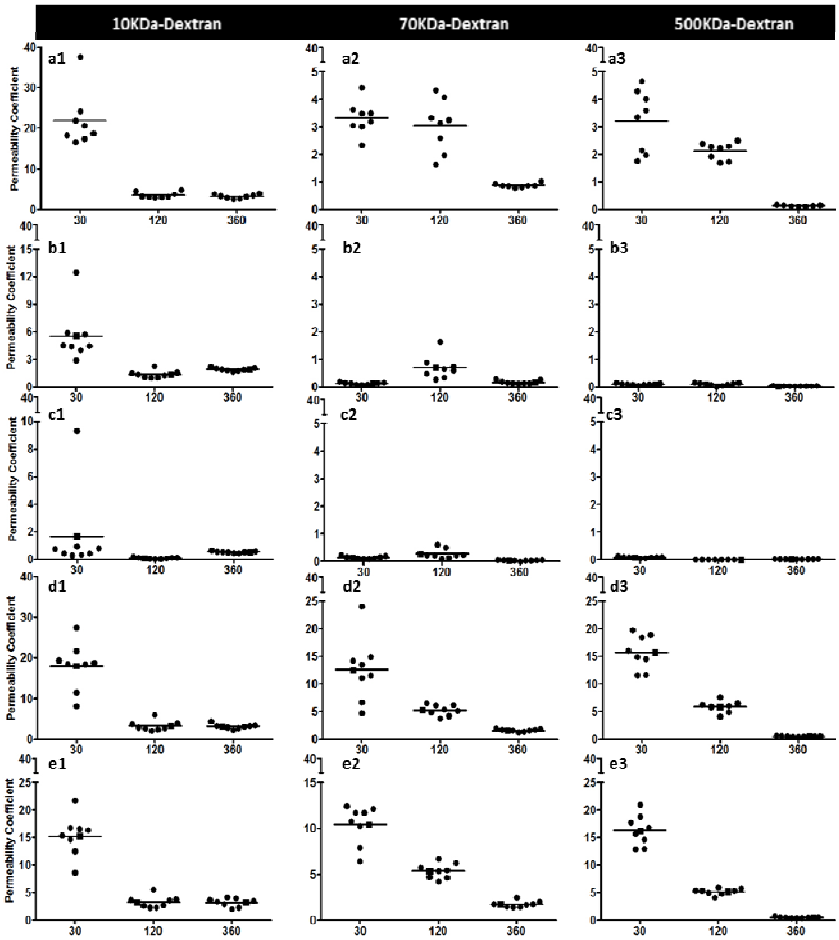

Figure 4b: Time dependent FITC-dextran permeability coefficients for a) alveolar epithelium, b) nasal epithelium, c) alveolar bilayer, d) A549 cell line and CRL-1848 cell line, at 30, 120, and 360 time intervals. The following permeability coefficient (P^K) equation was used to normalize the observed dextran data in Figure 5.

$P^K = (C_{dexB}/t)(1/A)(V_B/C_{dexA})$

A = tissue model surface area, C_{dexA} = apical dextran concentration, C_{dexB} = basal dextran concentration, t = time (sec), V_B = basal volume

* 1 denotes 10KDa, 2 denotes 70KDa, 3 denotes 500KDa FITC-Dextran

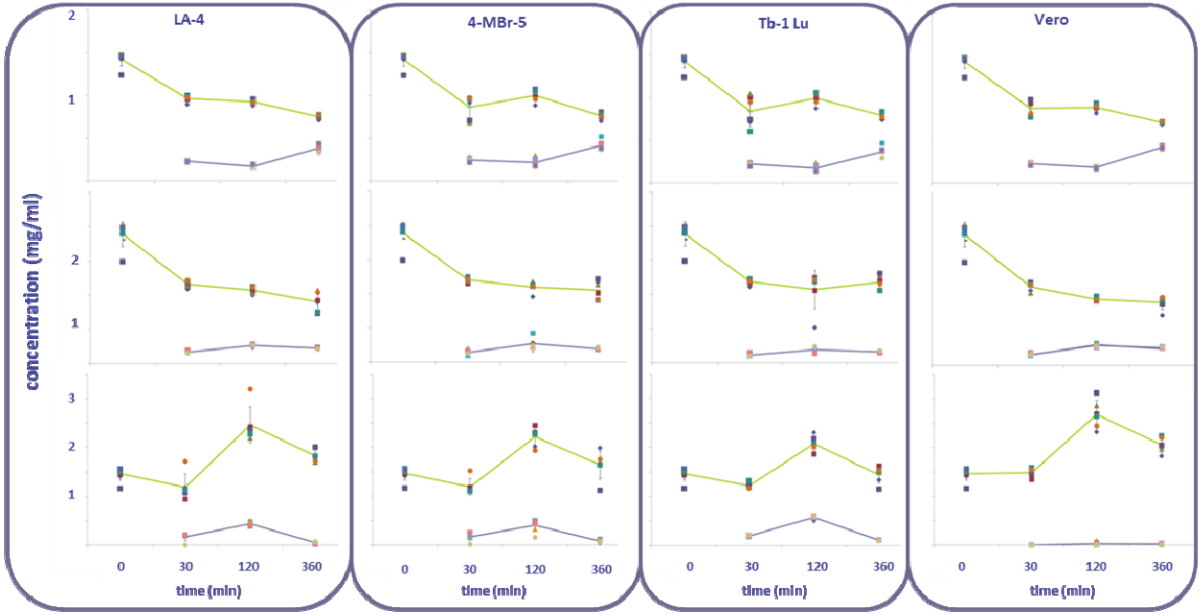

Figure 5: Kinetic quantification of FITC-dextran a) 10KDa, b) 70KDa, c) 500KDa concentration in the culture supernatant from non-human primate mucosal tissue models

* Green line denotes the quantified apical sample average from eight samples
* Blue line denotes the quantified basal sample average from eight samples

PART 2: *In vitro* aerosolized and liquid mode of respiratory antigen delivery in the humanized mucosal tissue equivalent

Introduction and Experimental Logic

The baseline barrier function work progressed into the evaluation of *in vitro* aerosolized delivery systems, with the humanized MTE modules. The logical progression of the work demonstrates the detection sensitivity of the *in vitro* aerosol delivery system, with the use of inert FITC-Dextran. The droplet size and the antigen molecular weight variables were directly compared to test the *in vitro* aerosol cloud application to the lung MTE. This was further tested with aerosolized influenza vaccine application, with the addition of select respiratory irritants including histamine. Here, the biological response serves as a measure of antigen delivery.

The lung MTE module exhibits distinctive transepithelial electrical resistance and permeability to cells and molecules of various molecular weight and size (2013 Annual Report, 2014 Quarterly Report 1). The aerosol application work builds on the barrier function understanding of the lung MTE tissue models and utilizes the VitroCell system for controlled aerosol generation *in vitro*. The real-time quantitative measure of aerosol mass deposition on the MTE demonstrates the system sensitivity for the 2.5-6um droplet delivery. Larger droplets of 4.5-6um were applied to the nasal MTE. Relatively smaller, 2.5-4um, droplets were applied to the alveolar MTE. The weight and size of the droplet deposition on the MTE was quantified with known concentrations of FITC-Dextran. The results show distinct differences between the size and weight of the droplets and this shows the system capability to generate biomimetic properties of the upper and lower airway. There was a detectable variation in the cloud deposition profiles with each molecular weight of antigen. This variation was anticipated in a dynamic delivery system with void space and variable cloud settling profiles. To this end, a series of respiratory antigen were applied in liquid and aerosolized phase, to compare the cellular response and the mode of antigen delivery. The results were evaluated in terms of dosimetery and innate cytokine and chemokine response with the addition of the immune cell components. Overall, the research findings demonstrate the feasibility of *in vitro* aerosol mode of antigen delivery and also demonstrate the need for extensive dosimetery studies. This system can be used alongside animal models to better understand or replicate some physiological processes associated withtemperature and droplet deposition range. The dosimetery of each antigen is recommended to directly compare the *in vitro* or *in vivo* cellular response.

The dynamics of aerosol deposition in the human airway is associated with the localized and systemic physiological response. There is a limited understanding of aerosolized deposition of live pathogen and the related local respiratory immunobiology. The quantitative measurement of droplet deposition for *in vitro* modeling of aerosol exposure may be relevant to human exposure to chemical and biological agents, but this is to be determined. Majority of *in vitro* model system are liquid phase (pipetted) antigen applications. This approach is valid with the assumption of 100% antigen delivery. The aerosolized application of antigen is a different process and depends on a number of dynamic processes including the concentration, weight,

size, flow rate. While this is a rather complex process, our study is a simplified iterative progression of the preliminary findings in aerosolized delivery of antigen to the lung MTE. We have found that aerosol delivery of antigen to the MTE does lead to immune responses, albeit with smaller responses than liquid delivery likely due to less antigen being delivered due to the inherent inefficiency of aerosol delivery as opposed to liquid pipetting. However, we do not know if aerosol delivery leads to an altered immune response as opposed to liquid delivery at this time. The feasibility of commercially available VitroCell Cloud system was tested with real-time mass transfer measurement of controlled droplets to the differentiated lung MTE modules. This simplified approach utilizes a vibration based nebulizer type of a set-up to a controlled exposure chamber. The differentiated lung tissue modules (MTE) are placed in the exposure chamber. An ultra-sensitive microbalance in the chamber measures real time mass deposition and the system records the antigen deposition process. This report describes our preliminary studies with the aerosolized mode of antigen delivery to the lung MTE and related tissue and immune cell response.

Dosimetery of FITC-Dextran in S1 Aerosol Droplet Size and Weight Measurement

Modeling environmental exposure to local respiratory mucosa is important for understanding aerosolized mode of therapeutic delivery and disease pathogenesis. The high throughput *in vitro* tissue engineering approach permits exhaustive interrogation of both antigen dosing and cellular response. This approach can be used to simplify the physiological complexity by step-wise introduction of physiologically relevant tissue factors and cells with kinetic introduction of antigen. In general, in vitro model antigen introduction is by liquid phase pipetting method. In comparison, little is known about the aerosolized mode of delivery for *in vitro* immunological studies. The instrumentation to mimic aerosolized exposure route is limited and it imposes various levels of experimental containment / safety. To this end, the VitroCell system is being studied for aerosolized antigen application to lung MTE. We initiated our studies with basic qualification of cloud measurement methods with controlled nebulized droplet size, to mimic the upper and lower airway exposure, with inert FITC-Dextran molecules of 10KDa, 70KDa, and 500KDa. The studies are intended to move closer towards *in vivo* physiological conditions and provide simplified methods and measures of droplet size and weight generation *in vitro.*

Aerosol Droplet Application of Respiratory Antigen

Our main objective is to develop 3D *in vitro* human mucosal models that mimic respiratory physiology and immunological function with common respiratory antigen related to influenza vaccine, bacterial and environmental antigen. The lung MTE is compartmentalized with the ability to mimic physiology by antigen capture and innate response at the mucosal interface, which recruits and primes antigen presenting cells (APC). The specialized APCs have the ability to travel to lymph nodes which are involved in a myriad of adaptive responses. The *in vitro* system is designed to mimic these physiological responses in a step-wise manner. These constructs help us better understand human immune responses to respiratory pathogens and environmental irritants and therapeutic vaccine formulations. Herein, we report the cytokine and chemokine response of aerosolized influenza vaccine antigen and inactive bacterial

bioparticle stimulation of the MTE with and without the addition of histamine. Under physiological conditions, histamine is synthesized by the decarboxylation of histadine and secreted when cells degranulate in response to antigen exposure. It is involved in a number of physiological processes with receptor mediated immunomodulation and suppression activity. There are four known histamine receptors (HR1, HR2, HR3, and HR4) are found on various cell types. HR1 and HR2 are present in airway endothelial and epithelial cells. HR1 is responsible for vasoconstriction and is associated with asthma, rhinitis and dermatitis. HR2 is responsible for antigen presenting cell based immunosuppression, resulting in inhibition of TH1 and TH2 response related to cytokine and antibody production. Thus, a combination of respiratory antigen with or without the addition of histamine may help identify the presence of HR1 or HR2 related cell based response, in the MTE model system. The following section summarizes the experimental set-ups.

Experimental Approach

Aerosol Droplet Size and Weight Measurement

Nasal and alveolar MTE were prepared as previously described (2013 Annual Report). VitroCell Cloud system (see Figure 1) was used for all the aerosol delivery studies. Stock concentration of 1mg/ml of FITC-dextran solutions of 10KDa, 70KDa and 500KDa were prepared in 1XDPBS and tested with 50ul multiple exposures. The machine nebulizer setting was adjusted for 4.5-6um to mimic the upper airway physiology, at 33^{o}C. The lower airway physiology was replicated with 2.5-4um nebulizer setting and 37^{o}C platform temperature. Fifteen replicate MTE modules were tested per condition to capture variance in the cloud based aerosol deposition. The microbalance and the exposure chamber were cleaned with 70% ethanol between each exposure. Real-time readouts were recorded and treatments were graphed based on the replicate exposure conditions.

Aerosol Droplet Application of Respiratory Antigen

Innate mucosal tissue response via aerosolized and liquid phase exposure to the lung mucosal tissue equivalent module (MTE)

2012-2013 FluMist® (live attenuated) and Fluzone® (split inactivated intramuscular) were tested at 1:500 dilution of the vaccine. *Staphylococcus Aureus* and *E Coli* bioparticles were tested at a concentration of 500K particles per ml. Histamine (Sigma) was tested at a 10pM concentration. For multiple exposures, histamine was applied to the MTE, via aerosol or liquid phase application. This was followed by the application of the respiratory antigen described above. All antigen formulations were prepared in X-Vivo media. The alveolar MTE was exposed to either small (2.5-4.0um) or relatively lower (4.5-6.5um) droplets, with multiple 50ul exposures. After one hour exposure, one million freshly thawed PBMC from eight donors were applied to the apical side of the MTE. This process mimics the recruitment of lymphocytes to an infected respiratory mucosal site. The apical side was washed after ninety minutes and the MTE modules were incubated overnight for monocyte extravasation through the tissue constructs.

The media from the receiving bucket was collected for multiplex cytokine and chemokine analysis. The cell adhesion protein related tissue factor will be reported in the next quarterly report.

Secretory cytokine and chemokine response

Millipore 16-plex kits were used to quantify the baseline tissue responses. The culture supernatants were diluted to 1:4 and 1:2 with X-vivo and tested along with kit standards and controls. The observed results are reported in concentration, picogram per milliliter.

a

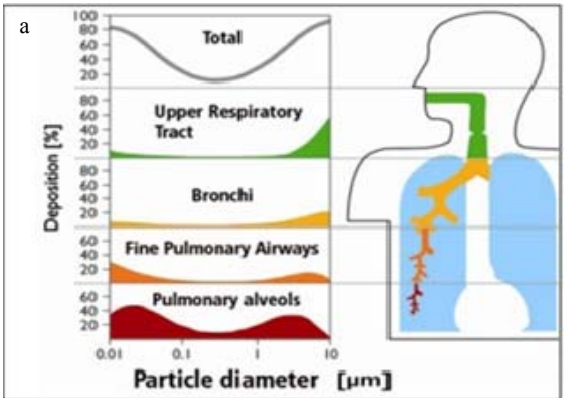

b

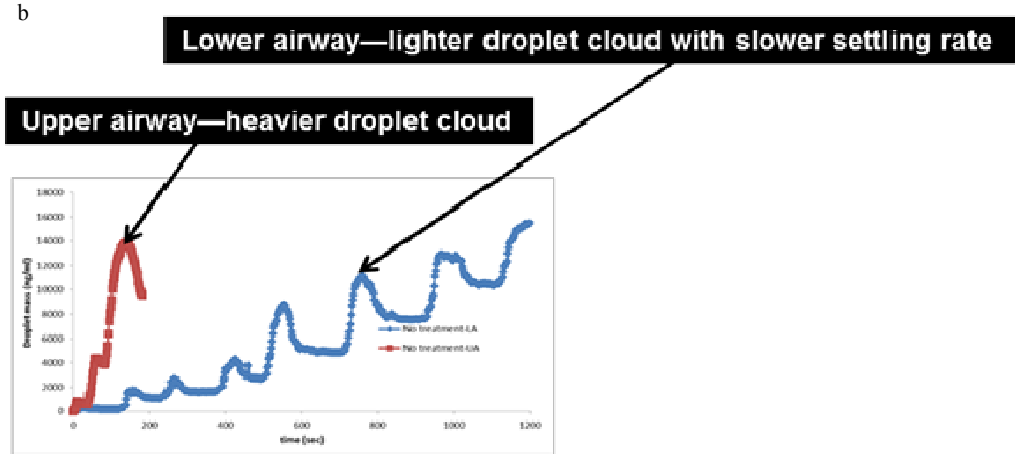

Figure 6: Comparison of In vivo and in vitro droplet profiles a) Farrell et. al. illustration of percentage droplet deposition correlations with various regions in the human airway, b) in vitro profiles of select droplet size ranges where 7-8 exposures of smaller droplet nebulization (ng/cm2) was comparable to 3 exposures with the larger droplets. The unloaded buffer solution produces a more defined cloud profile for both *in vitro* settings.

PART II: Results & Discussion

Basic Operation Review of Aerosol Exposure Chamber

The VitroCell Cloud system allows for exposure of up to 12 MTE modules (Figure 1). The cellular temperature at the time of exposure was controlled to mimic the upper airway (33^{o}C) and lower airway (37^{o}C) for the lower airway. The VitroCell Cloud system is fairly easy to operate. The nebulizer droplet size can be adjusted to mimic physiological conditions, where 2.5-4.0um size droplets were applied to the alveolar MTE and up to 4-6um size droplets were applied to the nasal MTE. The ultrasensitive crystal microbalance allowed for real-time measure of droplet deposition with the processor that connects to the computer software. The fluidics of the 2.5-6um aerosol exposure allows 0.1-0.3ml/min flow rates. Figure 2 shows representative profiles of aerosol deposition of base media. Here, multiple exposures of 50ul volume were applied per treatment and the data was recorded in real-time and normalized to time zero to adjust for the user application time-lag. The crystal microbalance needs to be replaced if broken, which results in irregular readouts. The system as a whole is autoclavable, as it is composed of medical grade stainless steel and plastic components. This system was tested inside a sterile hood. The chamber and the microbalance can also be wiped-down with 70% ethanol to clean the surfaces. We are in the process of testing an ultraporous open cube origami liner for the exposure chamber, as another safety measure. The lack of condensation effect in the cube chamber compared to the original VitroCell system makes it ideal for controlled droplet delivery with little to no accumulation of droplets that may result in overdose to the MTE. We are currently only using one microbalance. However, there is an option to connect multiple balances to the cube chamber. The system permits real-time readouts for the ambient air and exposure chamber. This can be used as a supplemental control and safety measure. Overall, this system is feasible for BSL2 lab work and needs to be somewhat modified for BSL3 or BSL4 labs.

Dosimetery of aerosolized FITC-Dextran to measure the effect of molecular weight and droplet size on MTE exposure

Inert FITC-dextran antigen solutions (1mg/ml) of 10KDa, 70KDa, 500KDa (Sigma) were prepared in 1XDPBS. The VitroCell system was set-up to collect real-time data at two second intervals. The MTE modules were placed in the exposure chamber after 2hr apical exposure to air. A series of fifteen readouts of FITC-Dextran application was collected per molecular weight exposure to measure the variance in cloud generation. The results for the 4-6um droplet cloud (mimicking the upper airway) show higher mass deposition, with molecular weight dependence. The lower airway MTE received smaller droplet application (2.5-4um). These results also show FITC-Dextran molecular weight dependence, with significantly lower droplet mass deposition. The results demonstrate that the system is biomimetic in nature, with a defined droplet range, and can be used for multiple exposure of select antigen. The physiological antigen deposition to the lower airway is an in-efficient process. Similarly, the amount of droplet antigen deposition to the lower MTE is less than half in mass per surface area (ng/cm2) when compared to the upper airway set-up. The system can be manually

adjusted to increase the droplet weight by simply altering the antigen solution concentration. This profile is similar to multiple respiratory exposures to environment irritants, pathogen, or therapeutic agents. The reference Figure 6a demonstrates the deposition efficiency in the localized respiratory regions as a guide for the expected physiological deposition range (Farrell, 2013). The VitroCell system captures parts of the physiological process, with tunable droplet size application with defined upper and lower respiratory temperatures.

Innate response of lung MT with aerosolized influenza vaccine antigen along with inactive bacterial and respiratory irritants

The real-time data from the aerosolized single and multiple MTE exposure to respiratory antigen shows an expected antigen dependent shift in the droplet mass deposition profiles. The aerosol exposure profiles of Flumist®, Fluzone®, inactive Staph Aureus bioparticles, and inactive E Coli bioparticles with and without the addition of histamine are shown in Appendix 1. The data is plotted side-by-side to compare the various exposure conditions relative to the no treatment control condition. Overall, the trends are similar to the FITC-Dextran study. They show altered weight of droplet size with the introduction of each type of antigen. For the vaccine formulations, this is the inactive or live attenuated influenza strain with its carrying vehicle alongside preservatives and adjuvant. There is less control over the size of inactive bacterial bioparticles in both the Staph Aureus and E Coli stocks, as these are irradiated antigen particles of various sizes. The mass deposition part of the study demonstrates the need to identify a representative droplet profile range for each antigen, to better understand the efficiency of the deposition process; see Appendix A as a reference to the variation in multiple antigen exposure profiles. The VitroCell nebulizer settings are arbitrary and can be adjusted to mimic the known *in vivo* physiological environment. The smaller (2.5-4um) and larger droplets (4.5-6um) clearly deposit different quantities of antigen in the system, with the same volume and concentration of starting material. The mass transfer profiles serve as a measure of liquid antigen droplets.

The MTE cellular response to various modes of antigen delivery shows the biological response associated with each method of delivery. Here, the innate response was characterized in terms of cytokine and chemokine production with aerosol vs. the liquid treatment. It is important to note that the MTE was sampled from the basal chamber where the extravagated monocytes or mature antigen presenting cells reside, after extravasation through the antigen exposed MTE. The MTE demonstrated a TH-1 (IL-12, TNF-alpha and IFN-gamma) and IL-10 immunosuppressive response from the addition of influenza vaccine antigen. However, the IL-10 response is more detectable in the liquid phase system due to higher antigen delivery dose. The pro-inflammatory cytokines IL-1a and IL-1b were also up-regulated with the addition of influenza antigen. This was coupled with MIP-1beta and G-CSF activity in the liquid phase application in the MTE. Overall, the MTE cytokine and chemokine response is in accord with influenza virus related innate response (McGill J, 2009). The 4.5-6um aerosolized droplets showed similar trends with lower secretory factor concentrations. The smaller droplets (2.5-4.5um) produced the mildest level of response above the no treatment control. This response is directly related to the efficiency of the aerosolized mode of antigen delivery. These findings are in agreement

with our previous reports with the alveolar MTE, where the response is both dose and influenza seasonal vaccine strain dependent. We chose to study the aerosol phase as it is the simplest, most direct, and natural method of antigen delivery (viral or therapeutic) to the lung mucosa in animals and humans, including military personnel. Note, however, that liquid delivery is the simplest, most direct route to a MTE construct. The MTE construct has been designed to be biomimetic with respect to cell phenotype, cell morphology, and immune and gene function to immune stimulants; however, it is not anatomically similar with respect to flow, tortuous pathways, geometries, etc. as are lung passages in humans. Thus, we are studying if aerosol delivery on a planar MTE surface has differential responses to liquid delivery. So far, we have found that aerosol delivery of Ag is less efficient than that of liquid delivery which is anticipated. To date, we have not found any feature that makes aerosol delivery unique with respect to a differential immune response, but more work needs to be done to assess if there are possible differentials. We hypothesize that the infection or challenge with a live virulent virus in the droplet phase may result in depot deposition and granuloma formation.

The immunosuppressive activity of histamine in the MTE was unexpected as it was initially expected to serve as a respiratory irritant, with HR1 type activity. However, the results demonstrate the primary role of antigen presenting cells in the overall immunosuppressive profiles of secretory cytokines and chemokines with the addition of synthetic histamine. This demonstrates that the immune cell activity and associated H2R response is predominant in the MTE. These findings correlate with H2R type of response, as reported by other research groups (Frei, 2013; Mazzoni, 2003). The only exception to this trend is the IL-12(p70) production in the alveolar MTE with the smaller droplet application. The results are graphed in Figures 9 shows side-by-side comparison of each mode of delivery. In general, the analytical scale for the liquid pipetted application is almost always higher than that of the aerosolized delivery. The low level of antigen delivery and the resultant modest immune response results from at least two factors: (1) to difference in droplet size as it relates to the antigen delivery dynamic in the *in vitro* cloud chamber and (2) we are able to determine the exact Ag dose that is being deposited on the MTE construct. Figure 9 demonstrates the sensitivity of the biological readout in each system. Here, the upper airway (2.5-4.5um droplet, 37^{o}C), lower airway (4.5-6.5um droplet, 33^{o}C) and liquid phase data is tabulated to show the strength of each system with direct comparison to the no treatment or histamine controls.

Overall, the MTE was able to produce a detectable biological response with single and multiple modes of aerosol delivery. The cloud phase application process is intrinsically different than the liquid phase delivery. There is a loss of antigen in the liquid to aerosol phase. However, the droplet mode of delivery is similar to *in vivo* respiratory tract infections, where depot effect and granulomas are common pathology readouts of infection and host immune response.

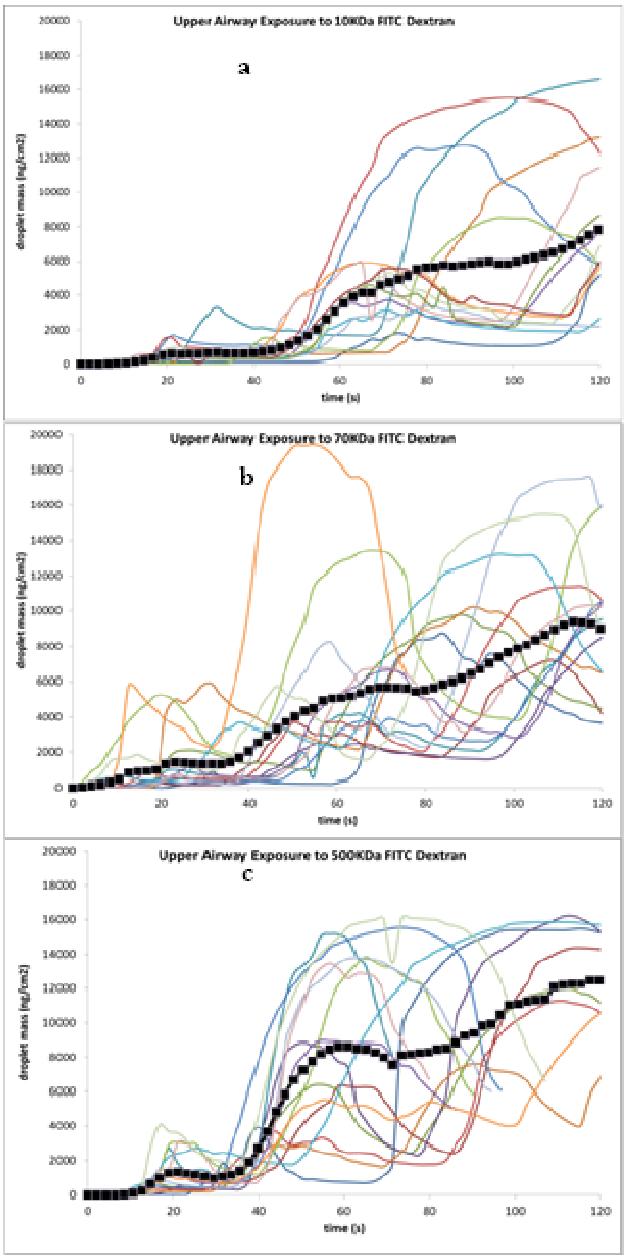

Figure 7: Upper airway MTE exposure (4-6um droplet cloud, 2sec per 2 min) a) 10KDa FITC-Dextran, b) 70KDa FITC-Dextran, c) 500KDa FITC Dextran. The real time data for the fifteen exposures per molecular weight are super-imposed. The black line shows the average trend for each antigen

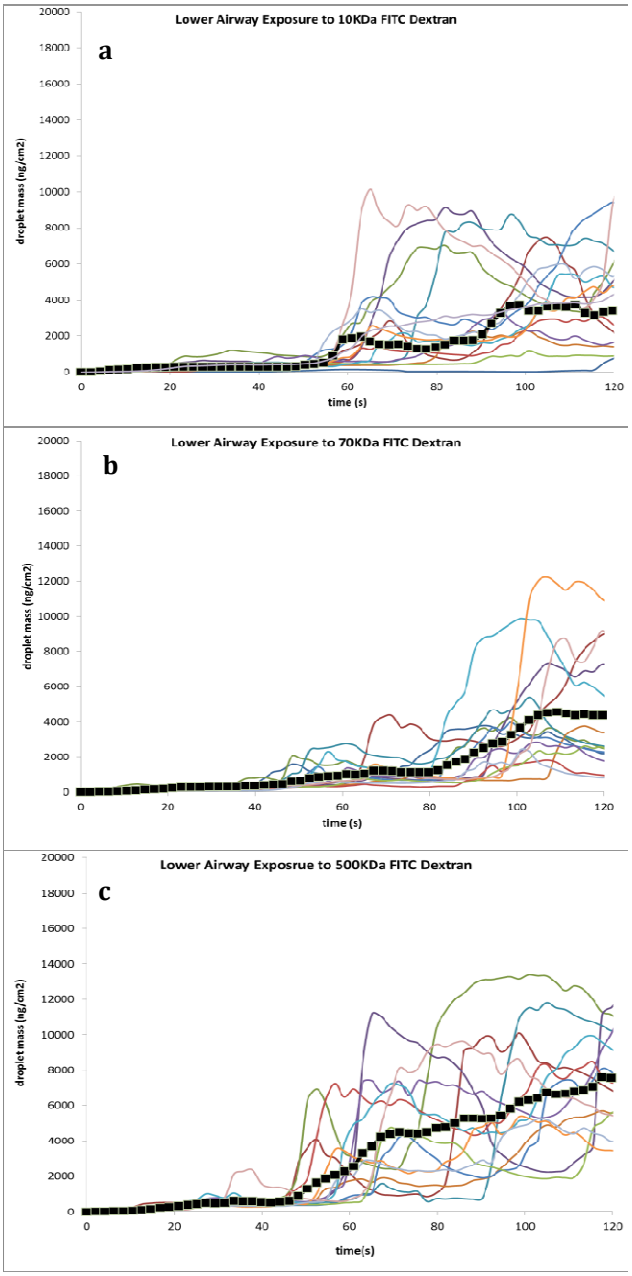

Figure 8: Lower airway MTE exposure (2.5-4um droplet cloud, 2 sec per 2 min) a) 10KDa FITC-dextran, b) 70KDa FITC-dextran, c) 500KDa FITC-dextran. The real time data for the fifteen exposure experiments are super-imposed. The black line shoes the average trend for each antigen

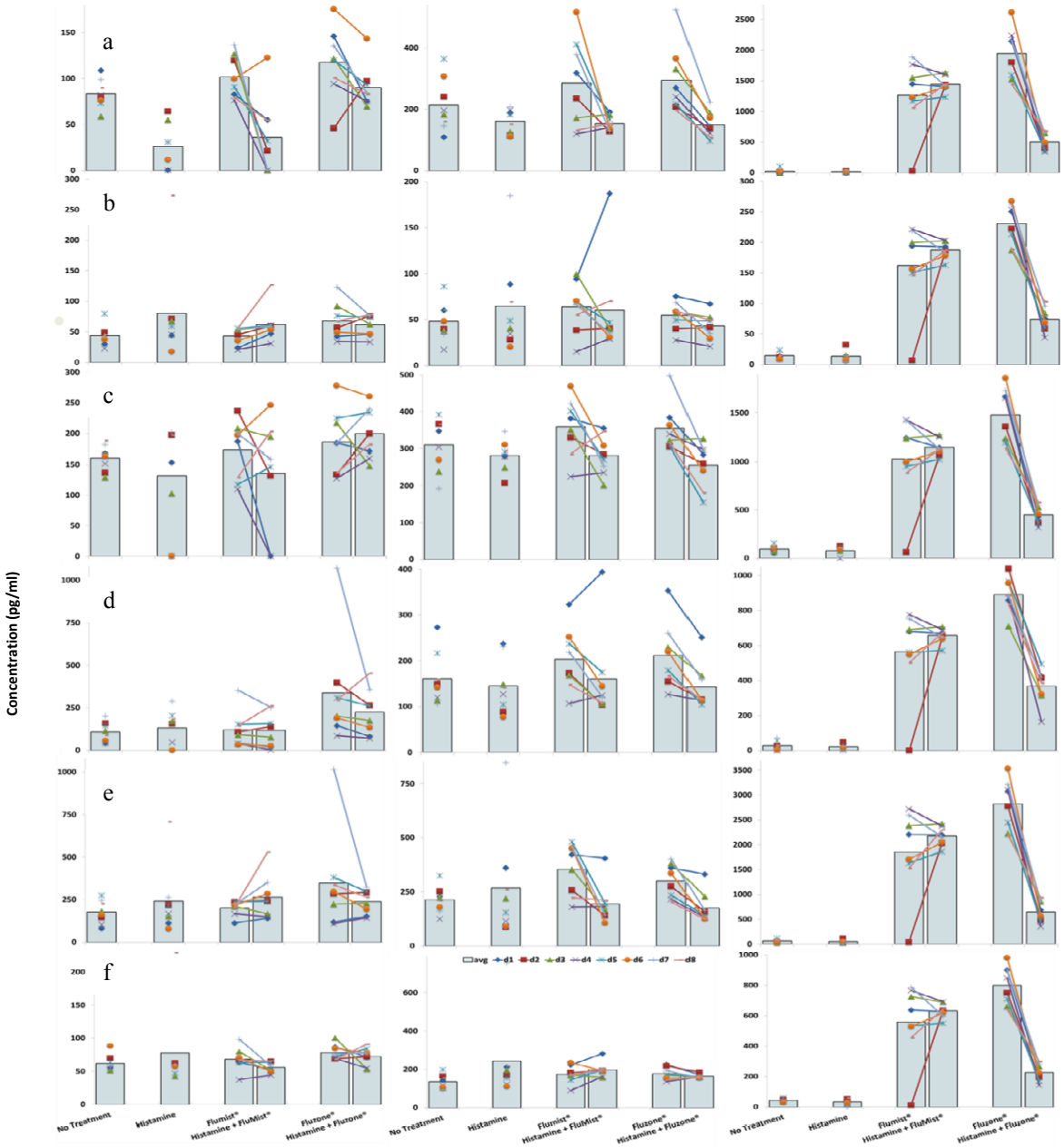

Figure 9b: Side-by-side comparison of cellular secretory cytokine and chemokine response to liquid and aerosol phase inactivated Fluzone® or live attenuated Flumist® multivalent vaccine with or without the addition of histamine on a donor basis a) IL-12(p40), b) TNF-alpha, c) IFN-alpha2, d) IFN-g, e) IL-10, f) IL-1a

PART 3: Evaluation of human MTE Cellular response to Inactivated and Live Attenuated Influenza Vaccine via Liquid and Aerosol Mode of Delivery

Introduction and Experimental logic

Influenza: basic pathology and vaccines

Influenza is one of the most common infectious pathogens known to humankind and therefore it is arguably the most studied pathogen by health and human services related agencies and pharmaceutical companies. The virus belongs to the Orthomyxoviridae family with four sub-types including A, B, C, and Thogotovirus. Both A and B subtypes are infectious in humans. The antigenicity of the A strain is dependent on two trans-membrane proteins designated as hemagglutinin (17 types) and neuraminidase (9 types), which serve as immunological targets with transient genetic shifts. On its own, influenza infection offers limited protective memory. The hemagglutinin and neuraminidase combinations from various species/regions of the world are closely tracked for the seasonal vaccine strain selection. Therefore, influenza vaccine is regularly reformulated, based on seasonal circulating strains in the human population. For example, H1 and H3 subtypes of influenza glycoprotein of human, swine and avian origin have been of interest in the past decade. The aerosolized mode of delivery is considered a natural viral entry pathway in the human airway. It is important to note that influenza infection and replication is directly associated with the respiratory tract. Both cellular and adaptive protective mechanisms are involved in clearing influenza infections. The droplet phase respiratory infection route generally begins with viral replication in the epithelial cells. The Type II epithelial cell is considered the primary viral infection target; although monocytes, macrophages and leukocytes can also be infected. The resulting cellular secretory factors are directly involved in neutrophil influx and antigen presenting cell recruitment from the local vasculature. These defense mechanisms can either mitigate or clear viral infection. The pro-inflammatory cytokines are of particular interest as they increase the vascular permeability, which leads to a systemic response. After inhalation of respiratory pathogen, the respiratory dendritic cells reside in the respiratory epithelium mobilize to the infection site, where majority of viral replication takes place. The transition from the innate response to adaptive immunity relies on professional antigen presenting cells, with capacity to activate naïve T cells. Whereas, CD8 T cell response is closely related to viral clearance related defense mechanisms including type I interferon response. While the innate response to influenza infection has been studied extensively, relatively little is known about the aerosolized mode of delivery and its role in priming the mucosal tissue during the preliminary introduction of viral antigen.

The aerosol delivery route in the airway is a natural and dynamic process that is dependent on a handful of major variables, including the type of antigen, its density and the delivery flow rate. Thus, these are some of the variables of interest for *in vitro* aerosol delivery systems. We have previously demonstrated the use of Vitrocell system to generate antigen clouds for direct application to the *in vitro* lung mucosal tissue constructs of upper and lower airway. In Part II, we described the evaluation of a tunable aerosol delivery system, where the antigen exposure and basic cellular response in terms of quantified cytokine and chemokine response to single or

multiple exposures to common respiratory antigen. These studies show the contribution of basic form and function of various cell type combinations in mucosal tissue equivalent constructs of human origin. In general, the primary human alveolar bilayer demonstrates enhanced biological function when compared against the epithelial-only model system. The focus of studies described in this report is limited to live attenuated Flumist® and inactivated Fluzone® vaccine with the addition of immune cell component. A pulmonary vascular endothelium tissue layer was added to the differentiated nasal epithelia, similar to the alveolar bilayer model. This model mimics a local tissue environment where the mucosal tissue is in direct contact with local vasculature. Based on our alveolar bilayer research findings, and *in vivo* immune-physiology, we have designed *in vitro* bilayer nasal mucosal model. The *in vitro* aerosol droplet size and temperature was controlled by altering the MTE temperature 33^{o}C and 4.5-6.4um droplets for the nasal mucosal MTE and 2.5-4.5um cloud at 37^{o}C for the lower airway MTE. The following section sums-up the effect of similar antigen to upper or lower airway lung models and their respective mode of delivery methods. For the influenza disease model, these *in vitro* lung MTE will be used for both *in vitro* vaccination and infection studies with recent influenza vaccine strains.

Our simplified *in vitro* mucosal tissue models mimics a cloud based antigen application in compartmentalized physiological regions of the airway. Live attenuated strains of the vaccine formulations were used, to safely work with relevant stains of influenza without the need for high biosafety level research facilities. This report focuses on nasal and alveolar bilayer tissue mucosal cellular response to the live attenuated intranasal Flumist® and inactivated intramuscular Fluzone® vaccine. The breakdown of the recent vaccine formulation components is listed below for clarity; Table 2.

Flumist®	Fluzone®
A/California/07/2009 (H1N1)	A/California/07/2009 (H1N1)
A/Texas/50/2012 (H3N2)--or--A/Victoria/361/2011	A/Texas/50/2012 (H3N2)--or--A/Victoria/361/2011
B/Yamagata/16/88--or--B/Massachusetts/2/2012	B/Yamagata/16/88--or--B/Massachusetts/2/2012
B/Victoria/2/87--or--B/Brisbane/60/2008	
monosodium glutamate	Formaldehyde
hydrolyzed procine gelatin	Octylphenol Ethoxylate
arginine	Thimerosol
sucrose	
dibasic potassium phosphate	
monobasic potassium phosphate	
ovalbumin	
gentamicin sulfate	

Table 2: Multivalent Live attenuated intranasal Flumist® and inactivated intramuscular Fluzone® formulations.

Our main objective is to develop biologically relevant 3D *in vitro* human mucosal models that mimic respiratory physiology and immunological function. The lung MTE is compartmentalized with the ability to mimic immuno-physiology by antigen capture and innate response with application at the mucosal interface. This design is similar to *in vivo* scenario, where the infected mucosal tissue recruits and primes the antigen presenting cells (APC). We take our

design inspiration from known function of the specialized APCs, which have the ability to travel to lymph nodes, involved in a myriad of adaptive responses. The mucosal site epithelia cells and the resident dendritic cells are directly involved in infection and disease pathogenesis. The MTE module design closely resembles these physiological pathways, in a step-wise manner. Our previous findings demonstrate superior function by the alveolar bilayer model consisting of airway endothelial cells alongside Type I and Type II epithelial cells. Here, the nasal mucosal model was matched with the alveolar bilayer model for direct comparison of cellular contribution to overall tissue response. This work is a prelude to direct infection with vaccinated MTE with wild-type strains. This ten-donor study directly compares the cellular response of aerosolized and liquid phase influenza vaccine application, in terms of antigen presenting cell maturation and secretory cytokine and chemokine response in the nasal and alveolar bilayer models.

Experimental Approach

Cell Culture

Primary human pulmonary nasal, alveolar and microvascular endothelial cells were purchased from PromoCell. The cells were passaged in T-175 tissue culture flasks. The primary tissue models were prepared by seeding 50,000 cells (passage 3) on a trans-well bucket coated with collagen and laminin in 10% serum containing 1:1 (v/v) Media199 and DMEM with 1% penicillin-streptomycin (sigma). After 3hr incubation, the multiwall plates were placed on the rocker at a rate of one cycle per minute. Media was exchanged every 48hr until the cells were confluent. The experiments were staggered to take into account the growth rates. The MTE were incubated without media for 3 hours, and then washed with 1XDPBS to remove any cellular debris, prior to cloud exposures.

Experimental treatments

The upper airway cloud was generated with the 4.5-6.0um VitroCell setting at 33^{o}C. The lower airway physiology was replicated with 2.5-4 um nebulizer setting and 37^{o}C platform temperature. The 2012-2013 FluMist® (live attenuated) and Fluzone® (inactivated intramuscular) were tested at 1:100 dilution of the vaccine. All influenza vaccine formulations were prepared in X-Vivo media and 50ul of either liquid or liquid-to-aerosol was tested over in two exposures. After one hour exposure, one million freshly thawed PBMC from ten donors were applied to the apical side of the nasal and alveolar MTE for ninety minutes. This process mimics the recruitment of lymphocytes to an infected respiratory mucosal site. The apical side was washed after ninety minutes and the MTE modules were incubated overnight for monocyte extravasation through the tissue constructs. The transmigrated cells were collected, from the receiving well, and stained for dendritic cell markers.

Cell surface marker expression and secretory cytokine and chemokine quantification

The antigen presenting cells were harvested from the receiving bucket and prepared for flow cytometry analysis. The cells were pelleted and stained for live-dead green and then stained with CD14-Alexafluir 750, HLA-DR PerCp-Cy5.5, CD80 APC, CD83 PE, CD86 and PE-Cy7. Flow cytometry analysis was performed on gated the live cell population.

Cytokine and Chemokine Quantification

The media from the receiving bucket was collected for multiplex cytokine and chemokine analysis. Millipore 16-plex kits were used to quantify the baseline tissue responses. The culture supernatants were diluted to 1:8,1:4 and 1:2 with X-vivo and tested along with kit standards and controls. The observed results are reported in concentration, picogram per milliliter. With the exception of IP-10, all data was plotted on a linear scale.

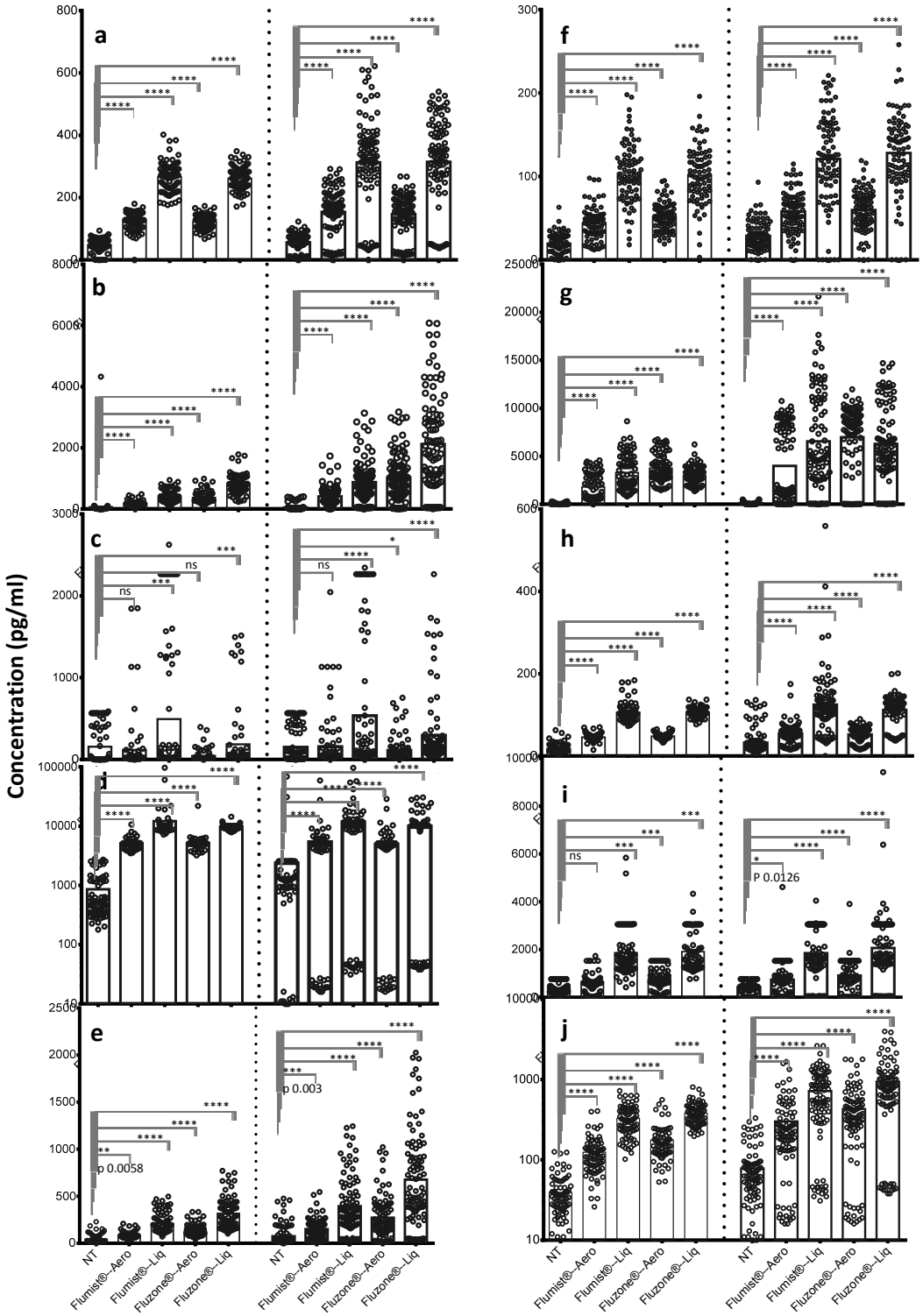

Figure 11: Multivalent influenza vaccine (live attenuated or inactivated) cytokine and chemokine response after aerosol or liquid phase exposure in the alveolar (right of dotted line) and nasal (left of dotted line) MTE a) IFN-alpha2, b) IFN-gamma, c) TNF-alpha, d) IP-10, e) IL-10, f) IL-12(P40), g) GM-CSF, h) IL-1alpha, i) IL-6, j) RANTES 1-way ANOVA was done using Kruskal-Wallis Test where ***p<0.001 and ns p >0.5

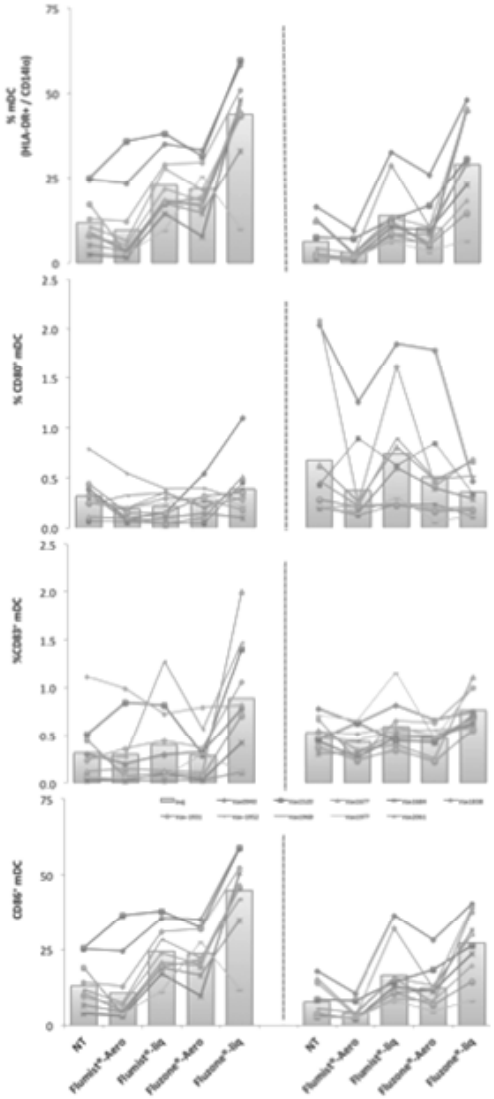

Figure 12: MTE derived antigen presenting cell surface marker expression of a) HLA-DR/CD14, b) CD80, c) CD86

PART 3: Results & Discussion

The aerosol biology work is of interest for understanding natural mode of disease pathogenesis and therapeutic development. There are multiple surveillance agencies actively working to create libraries of strains of graded virulence, each year. Influenza and filovirus strains are of current public and biothreat interest. Over the past three years, we have developed ten human and non-human primate simplified modular systems to explore the contribution of epithelial cells the localized immunological response. Our goal for the influenza disease model is to develop immunologically relevant *in vitro* respiratory tissue models for aerosolized antigen delivery and compare the standard liquid phase application with the aerosol mode of delivery. Based on the logical progression of relevant physiological readouts, we have selected the alveolar and nasal bilayer motif for the human influenza disease model. These modules are also being used for filovirus infection work at USAMRIID. We begin the discussion with a brief discussion of influenza and utility of live attenuated virus vaccine.

Influenza commonly circulates in the human population. The vaccines for influenza have been traditionally intramuscular and inactivated in nature. The aerosolized vaccination route is attractive for many reasons. This includes its similarity to natural viral infection, which results in both mucosal and systemic response against hemagglutinin and neuraminidase. This method can possibly eliminate the need and expense of a health care provider for vaccination. The degree of reactogenic response (runny nose, headaches, sore throat, muscle aches etc.) from self or healthcare provider administration has been shown to be comparable in a large-scale study (n=4651) (Ambrose, 2013). There has been considerable concern about virus shedding post vaccination and the potential risk for transmission immune compromised populations. The first report of viral shedding in human adults showed 50% positive virus shedding within in the first three days (Talbot, 2005) in 20 donors. There have been a number of more recent reports that 6-59 months of age have high as 79% viral shedding frequency (Mallory, 2011). The shedding rate for the 5-49 years of age is between 44-17%, with graduated reduction with relatively older populations (Block, 2008). This may partly be responsible for improved efficacy of live attenuated influenza vaccine in the elderly and children. In general, the live attenuated vaccines are tolerated in subjects of ≥2 years of age (Flumist® insert). Our interest in the live attenuated influenza vaccine (FluMist®) is based on its virus shedding characteristics and ease of use in BioSafety Level II labs. The intramuscular inactivated Fluzone® vaccine was tested as a comparative multivalent antigen to the Flumist®. We recognize the mismatch of the delivery route for the intramuscular inactivated Fluzone® vaccine respiratory mucosal tissue models. It is also important to note that the *in vitro* aerosolized antigen delivery is in its infancy stage and SPVD and our initial objective for a viral infection models are to compare liquid and aerosol modes of delivery through initial immunogenic response in the primary human alveolar and nasal mucosal modules. Table R5 demonstrates the sensitivity of the biological readout in each system. Here, the upper airway (2.5-4.5um droplet, 37^{o}C), lower airway (4.5-6.5um droplet, 33^{o}C) and liquid phase data is tabulated to show the strength of each system on its own, with direct comparison to the no treatment condition.

Both influenza and filovirus infection is initiated at the respiratory mucosal epithelium. The vascular endothelium plays a key role in mobilizing the local infection to a systemic immune response. Therefore, a number of iterations of influenza disease model are being developed for translating the science to *in vitro* modeling, which is appropriate for use in strain specific moderate to high biological safety labs. We have previously reported on superior performance of the simplified alveolar epithelium and endothelium bilayer model, when compared against the nasal or alveolar epithelium alone. The 2013 Annual Report demonstrates function in terms of permeability, vesicle cycling, gene expression, cytokine response and antigen presenting cell priming. This approach has been adapted to the nasal MTE with the addition of endothelial layer to improve the physiological relevance of the upper respiratory tract system in a similar manner. In Part II, we reported the cellular secretory cytokines and chemokine factors with tunable droplet mass in the alveolar mucosal tissue model. This work expands on the previous studies with the last iterations of the human upper and lower airway models. We have also started the process of adapting commercially available wild-type influenza virus strains to primary human cells, to move from vaccination to infection of the MTE.

The work builds on the permeability studies (Part I), which demonstrated the importance of a confluent endothelium for better barrier function by the human MTE modules. The transmigration of peripheral blood mononuclear cells through the tissue barrier is a natural selection process, known to drive dendritic cell differentiation. Thus, the final iteration for the upper and lower mucosal tissue equivalent model includes a confluent endothelium with an apical layer of differentiated nasal or alveolar epithelial cells. The nasal and alveolar MTE was treated with live attenuated influenza antigen in both liquid and aerosolized phase. The MTE temperature was carefully adjusted to known physiological conditions (33^{o}C for nasal and 37^{o}C for alveolar MTE). Similarly, the droplet size for the nasal MTE was relatively larger (4.5-6um) when compared against the alveolar MTE (2.5-4.5um). For future studies, we plan to work with USAMRIID to characterize the droplet size distribution and anticipate a Gaussian distribution range of the droplets. Compared to direct liquid application, the variation in the droplet size related inefficiency of antigen delivery is expected, as the physiological process itself is variable.

a

	Control	Nasal MTE sensitivity			
		Flumist®-Aerosolized	Flumist®-Liquid	Fluzone® -Aerosolized	Fluzone® -Liquid
IFN-alpha2	**relative to no treatment**	P<0.0001	P<0.0001	P<0.0001	P<0.0001
IFN-gamma	**relative to no treatment**	P<0.0001	P<0.0001	P<0.0001	P<0.0001
TNF-alpha	**relative to no treatment**	ns (p>0.5)	P<0.0001	ns (p>0.5)	P<0.0001
IP-10	**relative to no treatment**	P<0.0001	P<0.0001	P<0.0001	P<0.0001
IL-10	**relative to no treatment**	P<0.0001	P<0.0001	P<0.0001	P<0.0001
IL-12(p40)	**relative to no treatment**	P<0.0001	P<0.0001	P<0.0001	P<0.0001
GM-CSF	**relative to no treatment**	P<0.0001	P<0.0001	P<0.0001	P<0.0001
IL-1alpha	**relative to no treatment**	P<0.0001	P<0.0001	P<0.0001	P<0.0001
IL-6	**relative to no treatment**	ns (p>0.5)	P<0.0001	P<0.0001	P<0.0001
RANTES	**relative to no treatment**	P<0.0001	P<0.0001	P<0.0001	P<0.0001

b

	Control	Alveolar MTE sensitivity			
		Flumist®-Aerosolized	Flumist®-Liquid	Fluzone® -Aerosolized	Fluzone® -Liquid
IFN-alpha2	**relative to no treatment**	P<0.0001	P<0.0001	P<0.0001	P<0.0001
IFN-gamma	**relative to no treatment**	P<0.0001	P<0.0001	P<0.0001	P<0.0001
TNF-alpha	**relative to no treatment**	ns (p>0.5)	P<0.0001	P 0.01	P<0.0001
IP-10	**relative to no treatment**	P<0.0001	P<0.0001	P<0.0001	P<0.0001
IL-10	**relative to no treatment**	P<0.003	P<0.0001	P<0.0001	P<0.0001
IL-12(p40)	**relative to no treatment**	P<0.0001	P<0.0001	P<0.0001	P<0.0001
GM-CSF	**relative to no treatment**	P<0.0001	P<0.0001	P<0.0001	P<0.0001
IL-1alpha	**relative to no treatment**	P<0.0001	P<0.0001	P<0.0001	P<0.0001
IL-6	**relative to no treatment**	P 0.0126	P<0.0001	P<0.0001	P<0.0001
RANTES	**relative to no treatment**	P<0.0001	P<0.0001	P<0.0001	P<0.0001

Table R5: Tabulated relative MTE sensitivity based on relative p value of each model system a) nasal MTE with 4.5-6.0um droplet cloud aerosol application, b) 2.5-4.5um droplet cloud application

The live attenuated multivalent Flumist® influenza vaccine mildly infects the respiratory mucosa and is ideal for BSL 2 work. Here, we have shown its use in liquid and aerosol phase for direct comparison under select conditions that represent some basic variables in the local airway (described in the section above). We have demonstrated function in terms of cellular secretory factors including Interferon alpha2 and interferon gamma along with T cell activation marker RANTES, in the vaccinated tissue cultures (see Figure 11). The TNF-alpha response was mild or non-significant for the aerosolized mucosal constructs and showed more donor variation when compared against the IL-12(p40) profiles. In general, the nasal mucosal innate cellular cytokine response was slightly higher than that of alveolar tissue models, as shown in the Figure 11a, b, e, g, i. The IP-10 response was the only readout graphed on a log scale. This marker is a good indicator of infection, inflammation and is connected to the interferon gamma related response. There were some high and low responders for the live attenuated and inactivated vaccine antigen. In the nasal MTE, this trend was somewhat similar to RANTES, the other IFN-gamma related cytokine. The chemotactic cytokine GM-CSF levels were statistically higher in the nasal bilayer MTE with the Flumist® application. Surprisingly, the pro-inflammatory cytokines IL-1a and IL-6 levels were comparable in the alveolar and nasal MTE. These results do not resemble our previous findings with the differentiated nasal epithelium MTE (2013 Annual Report) and are likely related to the addition of the endothelial layer in the tissue motif. The alveolar MTE showed more dendritic cell maturation when compared against the nasal MTE, in terms of HLA-DR, CD14, and CD86 cell surface marker expression. Figure 12 shows the results for the alveolar and nasal MTE, from left to right of the dotted line respectively. In general, the stimulation index for Fluzone® was double than that of Flumist® for both liquid and aerosolized application. The liquid phase response was higher than the aerosol mode of delivery for both FluMist® and Fluzone®. There was more donor variation for CD80 and CD83. Altogether, the results show a higher degree of secretory cytokine and chemokine response in the nasal MTE and a slightly improved antigen presenting cell population in the alveolar MTE. We hypothesize that the cellular composition and associated secretory factors contribute to the overall MTE response. We hypothesize that the mucosal tissue cells from the upper airway may have relatively improved biological function in terms of secretory factors, as it is closer to environmental exposure. Whereas, the alveolar mucosal cells are in close contact with the dense vascular network, where immune cell recruitment and differentiation occurs. This ten-donor study demonstrates the similarity and differences in the upper and lower airway tissue with respect to antigen presenting cell maturation and cytokine and chemokine response. The viral infection related interferon alpha and gamma response trends were similar to RANTES profiles. Overall, the cellular secretory factor response was higher in the nasal MTE module. At first blush, this can simply be categorized as a high droplet mass and dose delivery scenario for the nasal MTE. However, the comparable pro-inflammatory IL-1alpha and IL-6 response demonstrates the independence of local tissue response to the droplet size for select biomarkers. We need to confirm the variation in the nasal and alveolar MTE with the use of more virulent viral strains. Future infection studies will be done with primary cell adapted influenza vaccine strains (shown in Table 2). The transition to wild-type strains will introduce cellular priming dose optimization and viability factors. We plan to pursue the antibody-assisted immunohistochemical staining of replicating virus in the MTE modules.

PART 4 Utility of commercially available peripheral blood mononuclear cells for use with MTE

Primary human peripheral blood mononuclear cells from three commercial sources (ZenBio Inc., StemCell Technologies, LifeTechnologies) were evaluated for use with the lung MTE module. The donations were purchased from each vendor and directly compared against cells obtained from the VaxDesign tissue bank, to characterize basic viability and cellular composition. Cells were tested on the day of arrival and immediately processed to reduce experimental variance due to freeze-thaw methodology.

Experimental Approach

Cellular viability and cell surface marker staining

Frozen cell pellets from three donors were purchased from LifeCell Technologies, StemCell Technologies, and VaxDesign Donor Bank. The vials were thawed in 37°C water bath. The cell suspension collected in warm (37°C), 5% pooled Ab media. The suspension was centrifuged at 300g for 10 minutes at room temperature (15 - 25°C). The viability was calculated by using trypan blue exclusion method by using a standard hemocytometer. The total cell density was based on the dilution factor and the number of live and dead cells. The cell pellets were re-suspended in $mIgG_1$ blocking buffer. After incubation (15min), they were re-suspended in Live Dead Green dye and the antibody cocktail for various cell surface markers including CD3, CD8, CD16, CD15, CD19, CD33, CD41a, and CD45. The cells were incubated for a half hour and then re-suspended in FACS buffer and then tested on a flow cytometer.

Results and Discussion

The direct comparison of PBMC sources showed a comparable degree of percent live cell population recovery from cells from ZenBio Inc., StemCell Technologies, LifeCell Technologies, and VaxDesign. However, the cell suspension density was variable and dependent on the commercial source. In general, the actual cell counts higher than the advertised cell density. This variable is cell batch dependent. Therefore, the percent viability was used a more reliable measure of overall PBMC recovery quality; Figure 6. The results demonstrate acceptable PBMC viability from all cell banks.

The cell suspensions were also tested for intrinsic levels of various cell types in the immune cell population. This assay serves as a secondary quality control measure of the donation and associated cell isolation method. Figure 7 shows the results for T cell, B cell, NK and monocyte ratios alongside platelet, granulocyte populations. The percent T and B cell composition was highest for the VaxDesign donations. In comparison, the ZenBio Inc. PBMC had the highest levels of NK cells, platelets and granulocytes. These contaminations are generally least desirable in our *in vitro* model systems. StemCell Technology donations had the highest level of monocytes. It is to be noted that the intrinsic donor make-up and quality of PBMC isolation method is detrimental to the level of monocytes in the final isolation. The subtitle differences in the PBMC cellular composition is attributed to the donor health and intrinsic cellular make-up.

We find all the commercially available cell sources feasible for *in vitro* tissue model work in conjunction with the MTE modules.

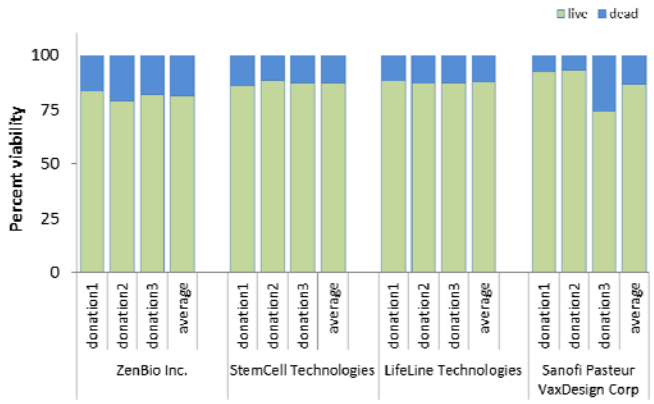

Figure 13: Percent viability of human peripheral blood mononuclear cells (n=3) from commercially available vendors

*ZenBio Inc. donations were fresh cell suspension
* StemCell Technologies, LifeLine Technologies, and VaxDesign blood bank donations were previously frozen

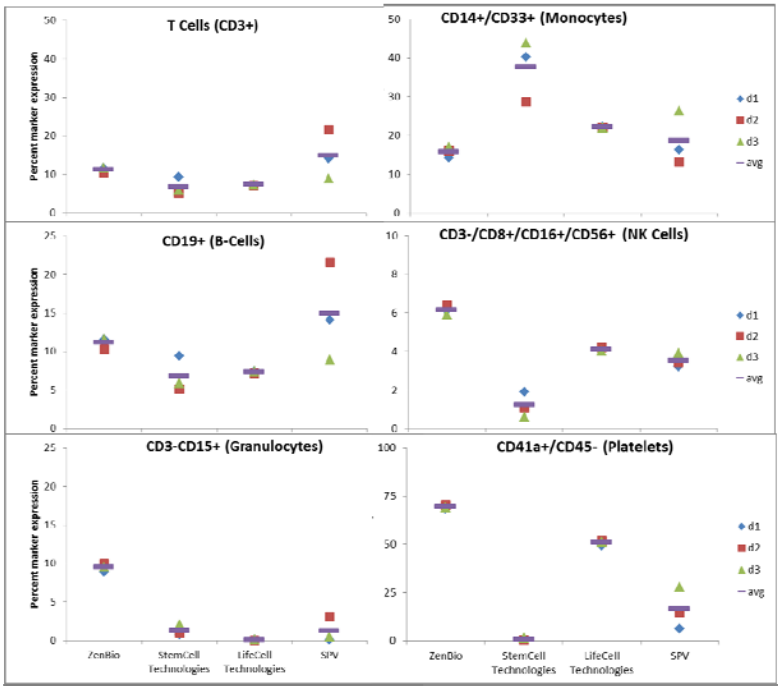

Figure 14: Cell surface maker expression of human perihpheral blood mononuclear cells

*ZenBio Inc. donations were fresh cell suspension
* StemCell Technologies, LifeLine Technologies, and VaxDesign blood bank donations were previously frozen

PART 5: Transfer of MTE module to USAMRIID

The MTE has been successfully shipped-out to USAMRIID labs and they have confirmed its viability and integrity on arrival. The alveolar MTE modules have also been successfully infected with Sudan and Ebola (SUDV, EBOV) filovirus strains. Based on positive findings and MTE infection with filovirus, we are proposing a fully vaccinated encapsulated MTE, with the immune cell component, for direct infection with BSL-IV grade virus infections at the Army Labs. The encapsulation work is novel to the Aerosolized Lung program. It is the most feasible option to transition into live infection studies. We recognize that there will be some developmental work needed for viable shipment of such a product. We plan to begin the studies with a portable incubator and gas pouches to mimic physiological conditions during the shipment process. This work will require a collaborative effort from both SPVD and USAMRIID for testing viability and function of the MTE product. To this end, we anticipate similar methodological program approach as shown in Table 1.

4. KEY RESEARCH ACCOMPLISHMENTS

PART 1: Baseline Barrier Function of Human and Non-Human Primate Tissue Models

A series of studies were designed to characterize the barrier function of in vitro human and non-human primate tissue models.

Transepithelial Resistance Method

- The primary human alveolar airway models exhibit high degree of stable tissue electrical resistance response and produce more consistent and reproducible results. The alveolar bilayer result is attributed to the addition of endothelium to the epithelial tissue, for the alveolar bilayer model. The nasal MTE was similar to the alveolar epithelium aloneMTE. The controlled growth rate and contact inhibition property of endothelium contributes to the confluence of the tissue layer. The nasal MTE was slightly less stable than the alveolar epithelial MTE. In comparison to primary MTE models, the A549 and CRL-1848 cell lines exhibited less consistent electrical resistance profiles with a higher degree of well-to-well variation. This result was somewhat anticipated, as most cell lines have higher cell growth rates, with a tendency for random cellular multilayer arrangement through low degree of cell-cell tight junction contact.

- The non-human primate cell line models showed similar resistance profiles to human cell lines. LA-4 and 4-MBr5 showed a stepwise increase in TEER over the seventy-two hour test period. This is indicative of cellular overgrowth. The Tb-1Lu cell line showed a decline in TEER. This relates to our previous findings with the gaps in tissue tight junctions leading to incomplete monolayer formation. Pervious cell staining studies showed that these cells tend to exhibit non-confluent layers of tissue. Of the NHP models, the Vero cell line showed the highest level of TEER stability. This is indicative of confluence in the tissue layer and controlled growth. However, this cell line is derived from African green monkey kidney tissue and therefore cannot be recommended for developing lung tissue models.

- The transepithelial resistance sensitivity was further tested by the addition of human peripheral blood monocytes with the addition of pro-inflammatory TNF-alpha or immunosuppressive dexamethasone. Overall, the addition of monocytes improved the electrical resistance. This increase in electrical resistance is likely due to the non-anchorage dependent cells “filling-out” the differentiated tissue layer during the cell adhesion step in monocyte extravasation process. This response resonates the high electrical resistance readouts by the multi-layer cell-line MTE models (with the exception of Vero cell line). The addition of dexamethasone resulted in a higher electrical resistance response for alveolar bilayer and A549 cell line. Whereas, a mild response was observed with nasal and alveolar epithelium alone MTE. In general, the basal TEER response to the nasal epithelium is not comparable to the level of response by the alveolar epithelium and the alveolar bilayer.

Pro-inflammatory TNF-alpha is known to induce mucosal leakiness, to facilitate leukocyte recruitment during innate response to infection. Similar to *other published findings* (Kataoka, 2002; Ge, 2009), all the MTE model systems showed a decline in TEER activity in response to TNF-alpha. Of the primary human models, the alveolar bilayer showed the highest level of response to immune mediators. A549 produced a higher electrical resistance response to immunopotentiators when compared to the bilayer model; however, its baseline level is relatively higher than the primary cell MTE models. In contrast, the CRL-1848 cell line showed the lowest level of activity. The results indicate that the basal cell line activity is not comparable to the primary human model systems. A side-by-side comparison of the MTE modules helps with generalized conclusions about the electrical resistance properties of the tissue with or without the addition of immune modulators and or immune cells demonstrates cell dependent barrier physiological response in the nine MTE model systems.

Molecular weight dependent FITC-dextran permeability

- The FITC dextran permeability results were in agreement with the TEER results (Part I) and our preliminary studies (2012-2013 Annual Report), in terms of alveolar bilayer stability and TEER response to immunopotentiators and permeability of inert dextran molecules. FITC dextran quantification in the various MTE modules showed least degree of permeation through the alveolar bilayer model for the human models. This result is in accord with the stable TEER findings in the previous section. A stable TEER readout is indicative of controlled growth rates and it is indirectly related to confluence. These studies also successfully captured the relative variation between the smallest molecular weight 10KDa FITC-dextran when compared against the 70KDa and 500KDa molecules for the alveolar and nasal epithelium alone MTE. All three molecular weight molecules of FITC-dextran were able to pass through the A549, CRL-1848, 4MBr5, and Tb-1Lu cell lines. This finding is directly related to cellular extravasation results (shown in 2012-2013 Annual Report). The level of FITC dextran permeability through the tissue models demonstrates the variation in primary cell and cell line MTE passive transport, where antigen presenting cell maturation, along with antigen and cellular transport related processes are critical for both innate and adaptive response.

PART 2: In vitro aerosolized and liquid mode of respiratory antigen delivery in the humanized mucosal tissue equivalent

Aerosol Droplet Size and Weight Measurement

- Our *in vitro* MTE aerosol model system can discriminate antigen in the range of 10-500KDa. The aerosolized FITC-Dextran application to the MTE shows a molecular weight dependence on the weight of the droplets (10KDa, 70KDa, 500KDa) for both the upper (2.5-4.5um) and lower (2.5um-4.5um) airway MTE.

- The *in vitro* model system can produce and detect aerosolized clouds of tunable droplet sizes and density. The dosimetery of FITC-Dextran of the lower airway (2.5-um-4.5um) is significantly lower than the upper airway (4.5-6.0). This demonstrates the sensitivity of the microbalance for the *in vitro* aerosol.

Aerosol Droplet Application of Respiratory Antigen

- Overall, the innate cytokine and chemokine response by the liquid application is significantly different than the aerosol mode of delivery. The results demonstrate the loss of antigen in the aerosol delivery process. It is different than the liquid phase application. However, the aerosolized antigen delivery process replicates *in vivo* respiratory biology based on simple design criterion like the droplet size range and infection temperature in the upper and lower airway.

- Using this model system, a broad range of antigen dosing will help better characterize the cellular response in a high throughput manner. Various motifs of both liquid and aerosol based application can be used to observe the biological response in replicate conditions. These *in vitro* studies permit numerous iterations of cellular and droplet delivery scenario when compared against the gold standard animal model systems.

- The innate response to the 2012-2013 influenza vaccine showed significant Th1 (IL-12, IFN and TNFalpha) response along with IL-10 related immunosuppressive activity above the no-treatment control. The IL-10 response is more discernible in the liquid phase (pipetted) system. In general, the liquid phase response was higher than the aerosolized mode of antigen delivery. It is important to note that both liquid and aerosol MTE mode of delivery are stand-alone systems.

- The innate response to inactive bacterial antigen was minor when compared against the influenza vaccine conditions. The response appears more pronounced in the 4.5-6.0um droplet application. This is mainly attributed to larger mass deposition with relatively larger droplets.

- The addition of histamine to the *in vitro* MTE cultures resulted in a suppressed cytokine and chemokine response. Similarly, the combination treatment of histamine and influenza vaccine and respiratory irritants reduced the innate cytokine and chemokine production. These findings are in accord with other *in vitro* histamine studies (Frei, 2013; Mazzoni, 2003) where the immune cells produce H2R related suppressive activity.

PART 3: Evaluation of human MTE Cellular response to Inactivated and Live Attenuated Influenza Vaccine via Liquid and Aerosol Mode of Delivery

The previous section demonstrated the efficacy of the VitroCell system for *in vitro* droplet phase delivery for a given antigen density and variable droplet size range. The preliminary

studies also compared the aerosolized antigen delivery and directly compared it to the liquid phase. For the influenza disease model, the focus was on *in vitro* influenza vaccination in the mucosal tissue equivalent (MTE) module, with aerosol and liquid phase application of live attenuated influenza Flumist® and inactivated intramuscular Fluzone® vaccine to both the *in vitro* nasal and alveolar endothelial/epithelial bilayer models. The commercially available live attenuated Flumist® is ideal for the current BSL2 facility at VaxDesign Campus of Sanofi, due to its live attenuated nature. For the last iteration of the MTE, both upper and lower respiratory MTE modules have been combined with respiratory microvascular endothelial cells to mimic the infected respiratory epithelial interaction with local vasculature and immune cells. The wild-type A and B influenza strains were adapted to primary human epithelial cells for live infection work. Similarly, the USAMRIID labs have demonstrated the utility of the lung MTE for live filovirus infections. For live viral disease models, we also plan to add-on the primed antigen presenting cells to the MTE modules for future studies pew minor adjustment in the current material transfer agreement to permit direct infection of the MTE for the filovirus work at USAMRIID labs.

A ten donor study of liquid and aerosolized antigen delivery showed quantifiable difference in cellular response in the various models. Here, multivalent live attenuated and inactivated influenza vaccines were tested in MTE with comparable cell types, under nasal or alveolar physiological conditions. The results demonstrate

- The selection of human nasal and alveolar bilayer model (epithelium and endothelium) as the last iteration of the infection mucosal tissue model. The bilayer endothelial and epithelial motif was designed to drive the transmigration process through the differentiated tissue layers. This work is a prelude to wild type live virus infection studies, where dendritic cells along with epithelial tissue are direct targets of filovirus and influenza infection.

- The direct comparison of nasal and alveolar bilayer models for influenza infection was done by comparing the multivalent intranasal attenuated vaccine Flumist®, with inactivated multivalent Fluzone® vaccine via liquid or aerosolized application, where the criteria matched with the local lung physiological parameters.

- Overall, the innate cytokine and chemokine response was higher in the nasal bilayer MTE, while the alveolar MTE showed an improved antigen presenting cell population. The interferon alpha and gamma response profiles were similar to RANTES and IP-10. These markers are indicative of preliminary cellular response to viral infection, albeit a mild version of the same. The pro-inflammatory cytokine response in the alveolar and nasal MTE was comparable and is attributed to the addition of the endothelial layer to the basic tissue motif, which provides better barrier function for selective transport processes, cellular differentiation and related local secretory factor secretion. Our results also demonstrate the expected and relatively milder cellular response via the aerosolized route for a fixed amount of starting material.

PART4: **Utility of commercially available peripheral blood mononuclear cells for use with MTE** ***and the Material Transfer Agreement adjustment***

Based on the discussion during a collaborator visit, a short study was designed to directly compare PBMCs from commercially availability cells from ZenBio Inc., StemCell Technologies, LifeCell Technologies. The results show that the viability of the PBMC from these commercial sources was comparable to VaxDesign products. The cellular composition of the donations was somewhat variable. This is an anticipated result since this criteria is dependent on donor cell population and cell isolation methodology. Overall, these preliminary results indicate any of the cell sources are feasible for use with the MTE modules.

PART 5: Transfer of MTE module to USAMRIID

- Four batches of alveolar and nasal MTE have been successfully transferred to USAMRIID Labs for live filovirus infections.

- The first three batches of MTE were shipped at room temperature. USAMRIID scientists have confirmed the viability and successful infection with SUDV and EBOV virus strains for up to nine days.

- Based on the success of this milestone, we have started the process of the addition of PBMC (from VaxDesign Blood Bank) to the MTA agreement.

- A portable incubator was used for the shipment of the last batch of MTE. This is the preferred method of delivery for the encapsulated MTE.

The next modified versions of the MTEs will include monocyte loaded mucosal tissue equivalent modules, based on the modified material transfer agreement. This work will require and iterative approach (similar to the initial MTE transfer) by both USAMRIID and SPVD labs to confirm the viability and function of the live tissue product.

5. OVERALL CONCLUSIONS

This report summarizes a series studies to quantify barrier function of human and non-human primate tissue models, as the work transitions into aerosolized delivery systems, where the response was measured as a function of dose and some biological and innate immunological functions. Stable TEER readouts and impermeability of FITC-dextran in the alveolar bilayer model demonstrates the tissue confluence and improved cell-cell contact in the cellular layers. This function also drives active cellular extravasation processes. Based on difference in primary cell and cell line results, we anticipate each of the human and non-human primate models to possess its own intrinsic barrier functional properties. The alveolar bilayer model showed relatively higher degree of controlled barrier function when directly compared against human and non-human primate tissue models. Increased permeability, leukocyte recruitment and plasma leakage is related to intrinsic tissue tight junction proteins and the junction-intracellular enzymatic and energetic pathways. These processes are evoked by hyper-permeability mediators like histamine, thrombin, leukotrienes and cytokines. These biological mediators directly interact with the cell surface molecules and tight junction proteins. Primary cells from nasal epithelium and the lower airway alveolar region have intrinsic differences in cell-surface and tight junction protein interactions (Kumar 2009). Thus, the primary cells and cell lines are expected to have differences in cell-cell and cell-substrate interactions.

Overall, the barrier function related studies are in accord with our previous work related to airway tissue integrity (shown in summary Table 1). The transepithelial resistance studies and FITC-dextran permeability work show agreement with each other and demonstrate the differences between primary cell line containing mucosal tissue modules composed of human and non-human primate cells. We anticipate that the TEER method and FITC labeled dextran mass transfer studies both serve as quantifiable methods to work with both homogenous and aerosolized antigen delivery systems. We hypothesize that the concentration and type of antigen delivery will produce a variable response in the primary cell and cell lines of human and non-human primate origin.

After the barrier function studies, the focus of the work transitioned to humanized MTE models and mode of delivery. The preliminary results from the *in vitro* aerosolized delivery experiments demonstrate the feasibility of the VitroCell Cloud system with the MTE module of the MIMIC® settings. The mass transfer profile differentials between the upper and lower airway droplet profiles show the capability of the nebulizer to generate droplets of 2.5-6um size and weight. The variable molecular weight FITC dextran studies show the sensitivity of the system for measuring droplet mass to a given surface area. On a similar note, the influenza vaccine, bacterial antigen and histamine introduction showed significant shift in mass transfer profiles, when compared against the no treatment control. Similarly, the simplicity and the known molecular size of the FITC-Dextran application studies made them ideal for testing the system detection capability. The system is capable of differentiating between the upper and lower airway droplet setting. However, the response for each antigen or drug formulation needs to be fine-tuned to identify a distribution of cloud size. More work needs to be performed on the aerosol delivery to assess appropriateness with in vitro tissue constructs. .

The Th1/Th2 response from the influenza vaccine antigen demonstrates the biological responsiveness to aerosolized application. The mode of delivery was assessed in terms of identical antigen preps directly pipetted to the MTE, to replicate the standard *in vitro* antigen application method. In general, the degree of response from the aerosolized delivery is much lower than that of liquid application. This is an anticipated inefficiency, as the nebulization process exposes more than just the MTE module area to the cloud droplets. The results show the role of antigen dose and the mode of antigen delivery in producing a dose dependent biological response. It is also important to note the difference in no treatment response (base media) between the liquid and aerosol phase delivery. The aerosol phase base line response is more variable and in some cases higher than that of the liquid phase application.

The purpose of the histamine exposure study was to capture the effects of multiple aerosolized antigen deposition in terms of mass transfer and cellular response, with the VitroCell System. The system does detect variations in the cloud generation profiles with multiple exposures of the same or different types of antigen. The histamine exposure results show HR2 activity in the MTE basal chamber. The response can be attributed to the extravasated antigen presenting cells in the basal chamber. The histamine antigen associated immunosuppressive results are in accord with other published findings with sorted plasmacytoid dendritic cells or other antigen presenting cell populations (Frei, 2013; Mazzoni, 2003). The H2R associated histamine response demonstrates the variation in degree of response based on the delivered antigen does. To better understand the droplet profiles as it relates to total antigen delivery, we are in the process of screening particle sizer instrument. This method will provide a secondary measure of droplet profiles with single or multiple antigen exposures.

The last iteration of the MTE, with primary human endothelial and epithelial cells, has been selected for future infection studies for the *in vitro* mucosal tissue models. To simplify complex physiology to biologically relevant variables including the MTE cell type, antigen droplet size and physiological temperature, for the aerosolized MTE application. The amount of baseline response by no treatment condition defines the sensitivity of the detected biological response by the differentiated mucosa at the air liquid interface alone. We anticipate cellular and biological differences in the liquid and aerosol mode of delivery based on these biological knowns and the experimental findings support the hypothesis. This ten-donor study demonstrates the similarity and differences in the upper and lower airway MTE with respect to antigen presenting cell maturation and cytokine and chemokine response. The viral infection related interferon alpha and gamma response trends were similar to RANTES profiles. Overall, the cellular secretory factor response was higher in the nasal MTE module. At first blush, this can simply be categorized as a high droplet mass and dose delivery scenario for the nasal MTE. However, the comparable pro-inflammatory IL-1alpha and IL-6 response demonstrates the independence of local tissue response to the droplet size for select biomarkers. This demonstrates the overall contribution of cell types in the differentiated MTE tissue.

The next step for the influenza disease model is to transition to wild-type infection with Influenza A/California/07/2009, A/Texas/50/2012, B/Yamagata/16/88, and

B/Victoria/2/87/2008 and begin antibody assisted plaque assay and/or qPCR methods to quantify the infection. Overall, the Aerosolized lung project is moving forward with the accomplishment of our proposed milestones. We plan to introduce T and B cell based co-culture assays in the next phase of the influenza disease model. The encapsulated MTE work will begin after the execution of the modified MTA. We look forward to testing therapeutics or other biologics to further develop the *in vitro* lung model systems for filovirus infection.

6. PUBLICATIONS, ABSTRACTS, AND PRESENTATIONS

Mahmood A, Bailey V, Warren W, Dye J, Design and Evaluation of *In Vitro* Lung Tissue Models for Antigen Delivery Transactions of the Society For Biomaterials April 2014

Mahmood A, Dye J *In Vitro* Aerosolized Antigen Dosimetry Lung Models Annual American Association of Aerosol Research Meeting 2014, Orlando, Florida

Mahmood A, Dye J Immune response to respiratory antigen in the Mucosal Tissue Equivalent Model Tissue Engineering and Regenerative Medicine International Society 2014, Washington DC (*Accepted*).

Brannan, J , Mahmood A, Kuehne A, Dye, J, Novel *in vitro / ex vivo* animal modeling for filovirus aerosol infection using the MIMIC® system, 2014 Chemical and Biological Defense Science & Technology Conference, St. Louis, MO

7. INVENTIONS, PATENTS and LICENSES

There were no inventions, patents or licenses filed for the 2013-2014 fiscal year.

8. REPORTABLE OUTCOMES

The human alveolar and nasal MTE product has been successfully shipped out to USAMRIID labs. This model system can be used to test the infection susceptibility of infectious agents. This viable tissue model has been tested at USAMRIID labs for live filovirus infections. Thus far, SUDV and EBOV strains have been tested using the human MTE. This work is limited to liquid phase antigen delivery. The SPVD work related to in vitro influenza antigen delivery can be translated to testing droplet phase filovirus therapeutic delivery and infection models. We anticipate further development of the system with the addition of immune cells.

9. OTHER ACHIEVEMENTS

Nothing to Report.

10. REFERENCES

Ambrose CS1, Wu X. The safety and effectiveness of self-administration of intranasal live attenuated influenza vaccine in adults. Vaccine. 2013 Jan 30;31(6):857-60.

Armstrong SM, Wang C, Tigdi J, Si X, Dumpit C, Charles S, Gamage A, Moraes TJ, Lee WL. Influenza infects lung microvascular endothelium leading to microvascular leak: role of apoptosis and claudin-5. PLoS One. 2012;7(10):e47323.

Bayat S, Anglade D, Menaouar A, Martiel JL, Lafond JL, Benchetrit G, Grimbert FA, *In vivo* measurement of lung capillary-alveolar macromolecule permeability by saturation bronchoalveolar lavage, Crit Care Med 2000 Aug; 28(8):2937-42.

Benson K, Cramer S, Galla HJ. Impedance-based cell monitoring: barrier properties and beyond. Fluids Barriers CNS. 2013 Jan 10;10(1):5.

Block SL1, Yogev R, Hayden FG, Ambrose CS, Zeng W, Walker RE. Shedding and immunogenicity of live attenuated influenza vaccine virus in subjects 5-49 years of age. Vaccine. 2008 Sep 8;26(38):4940-6

Briot R, Bayat S, Anglade D, Martiel JL, Grimbert F, Monitoring the capillary-alveolar leakage in an A.R.D.S. model using broncho-alveolar lavage, Mircrocirculation, 2008 April; 15(3):237-49.

Farrell G ICAO Information Paper CAEP-SG/ 20082-IP/05 CSIEO 12/472, 2013.

Fischbarg J. Fluid transport across leaky epithelia: central role of the tight junction and supporting role of aquaporins. Physiol Rev. 2010 Oct;90(4):1271-90.

FluMist® Product Insert
http://www.fda.gov/downloads/BiologicsBloodVaccines/Vaccines/ApprovedProducts/ucm294307.pdf

Frei R1, Ferstl R, Konieczna P, Ziegler M, Simon T, Rugeles TM, Mailand S, Watanabe T, Lauener R, Akdis CA,

Ge Y, Deng T, Zheng X. Dynamic monitoring of changes in endothelial cell-substrate adhesiveness during leukocyte adhesion by microelectrical impedance assay. Acta Biochim Biophys Sin 2009 Mar;41(3):256-62.

Grommes J, Soehnlein O. Contribution of neutrophils to acute lung injury. Mol Med. 2011 Mar-Apr;17(3-4):293-307.

Gurey BP, Nelson S, Viget N, Fialdes P, Summer WR, Dobard E, Beaucaire G, Mason CM, Flu0rescein-labeled dextran concentration is increased in BAL fluid after ANTU-induced edema, J Appl Physiol, 1998 Sept; 85(3):842-8.

Jefferson TO, Rivetti D, Di Pietrantonj C, Rivetti A, Demicheli V. Vaccines for preventing influenza in healthy adults. Cochrane Database Syst Rev. 2007 Apr 18;(2):CD001269.

Jefferson T1, Rivetti A, Di Pietrantonj C, Demicheli V, Ferroni E. Vaccines for preventing influenza in healthy children. Cochrane Database Syst Rev. 2012 Aug 15;8:CD004879.

Jutel M1, Akdis M, Akdis CA. Histamine, histamine receptors and their role in immune pathology. Clin Exp Allergy. 2009 Dec;39(12):1786-800.

Kreijtz JH, Fouchier RA, Rimmelzwaan GF Immune responses to influenza virus infection. Virus Res. 2011 Dec;162(1-2):19-30.

Kataoka N, Iwaki K, Hashimoto K, Mochizuki S, Ogasawara Y, Sato M, Tsujioka K, Kajiya F. Measurements of endothelial cell-to-cell and cell-to-substrate gaps and micromechanical properties of endothelial cells during monocyte adhesion. Proc Natl Acad Sci U S A. 2002 Nov 26;99(24):15638-43.

Kumar P, Shen Q, Pivetti CD, Lee ES, Wu MH, Yuan SY. Molecular mechanisms of endothelial hyperpermeability: implications in inflammation. Expert Rev Mol Med. 2009 Jun 30;11:e19.

Mallory RM1, Yi T, Ambrose CS. Shedding of Ann Arbor strain live attenuated influenza vaccine virus in children 6-59 months of age. Vaccine. 2011 Jun 10;29(26):4322-7.

Mazzoni A1, Leifer CA, Mullen GE, Kennedy MN, Klinman DM, Segal DM. Cutting edge: histamine inhibits IFN-alpha release from plasmacytoid dendritic cells. J Immunol. 2003 Mar 1;170(5):2269-73.
McGill J1, Heusel JW, Legge KL. Innate immune control and regulation of influenza virus infections. J Leukoc Biol. 2009 Oct;86(4):803-12.

McGill J1, Heusel JW, Legge KL. Innate immune control and regulation of influenza virus infections. J Leukoc Biol. 2009 Oct;86(4):803-12.

O'Mahony L. Histamine receptor 2 modifies dendritic cell responses to microbial ligands. J Allergy Clin Immunol. 2013 Jul;132(1):194-204.

Sedgwick JB, Menon I, Gern JE, Busse WW. Effects of inflammatory cytokines on the permeability of human lung microvascular endothelial cell monolayers and differential eosinophil transmigration. J Allergy Clin Immunol. 2002 Nov;110(5):752-6.

Talbot TR1, Crocker DD, Peters J, Doersam JK, Ikizler MR, Sannella E, Wright PE, Edwards KM. Duration of virus shedding after trivalent intranasal live attenuated influenza vaccination in adults. Infect Control Hosp Epidemiol. 2005 May;26(5):494-500.

11. APPENDICES

Figure A1: Aerosolized dosimetery on upper and lower airway with Flumist® antigen

Figure A2: Aerosolized dosimetery on upper and lower airway with Fluzone® antigen

Figure A3: Aerosolized dosimetery on upper and lower airway with Staphylococcus Aureus antigen

Figure A4: Aerosolized dosimetery on upper and lower airway with e coli bioparticles antigen

Figure A5: Aerosolized dosimetery on upper and lower airway with histamine antigen

Figure A6: Aerosolized dosimetery on upper and lower airway with histamine plus Flumist® antigen

Figure A7: Aerosolized dosimetery on upper and lower airway with histamine plus Fluzone® antigen

Figure A8: Aerosolized dosimetery on upper and lower airway with histamine plus staphylococcus Aureus bioparticles antigen

Figure A9: Aerosolized dosimetery on upper and lower airway with histamine plus e coli bioparticles antigen

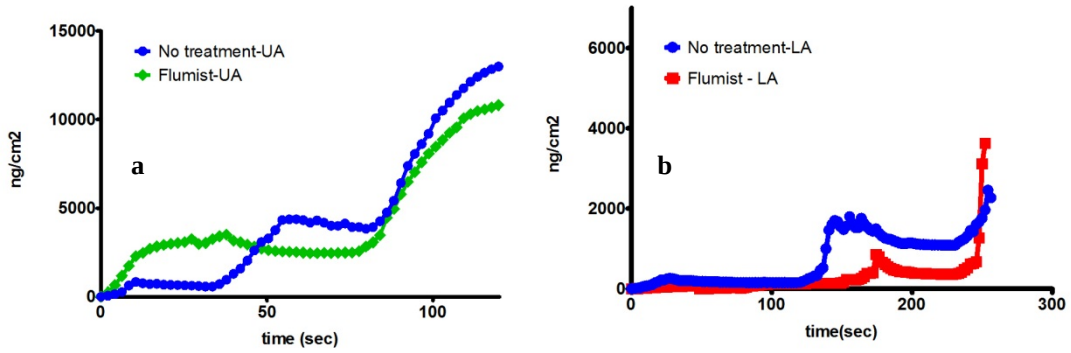

Figure A1: Aerosolized dosimetery on upper and lower airway with Flumist® antigen

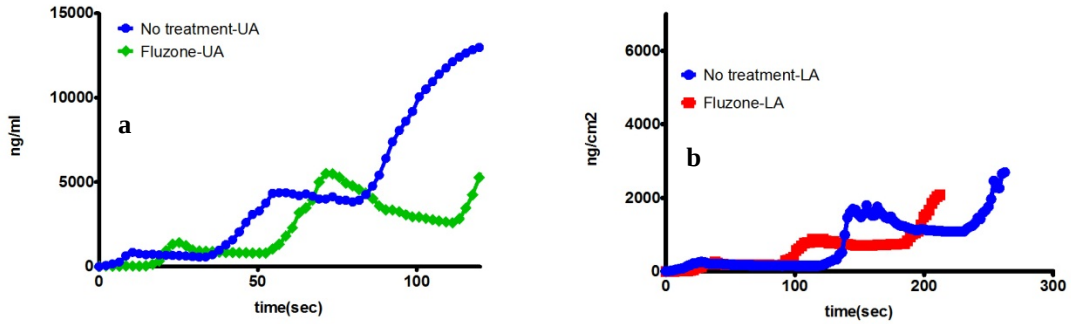

Figure A2: Aerosolized dosimetery on upper and lower airway with Fluzone® antigen

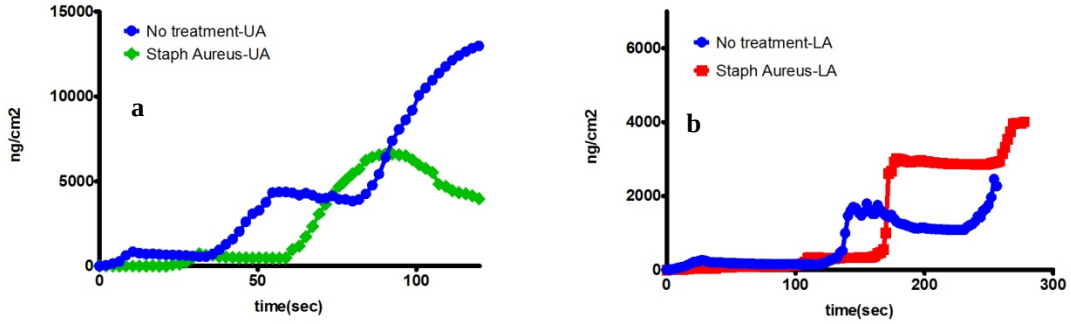

Figure A3: Aerosolized dosimetery on upper and lower airway with Staphylococcus Aureus antigen

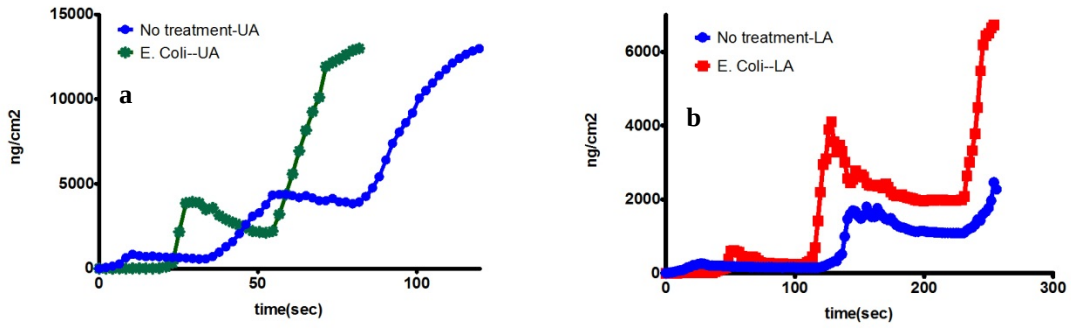

Figure A4: Aerosolized dosimetery on upper and lower airway with e coli bioparticles antigen

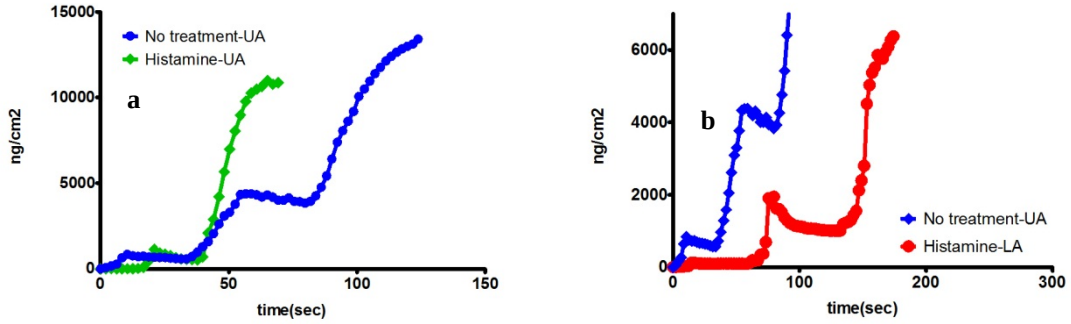

Figure A5: Aerosolized dosimetery on upper and lower airway with histamine antigen

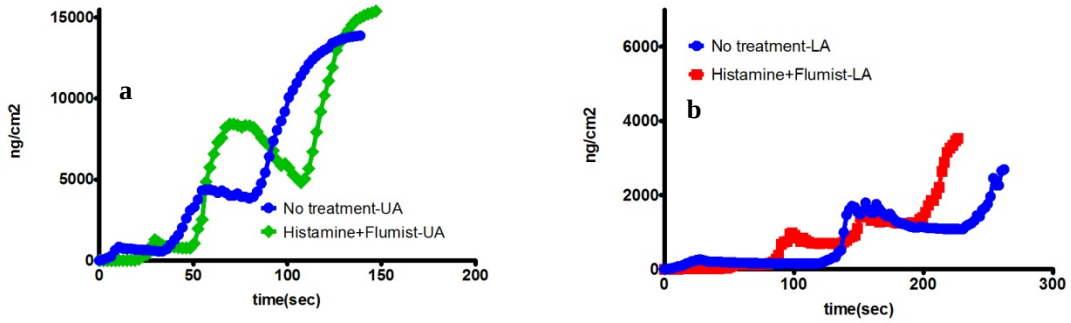

Figure A6: Aerosolized dosimetery on upper and lower airway with histamine plus Flumist® antigen

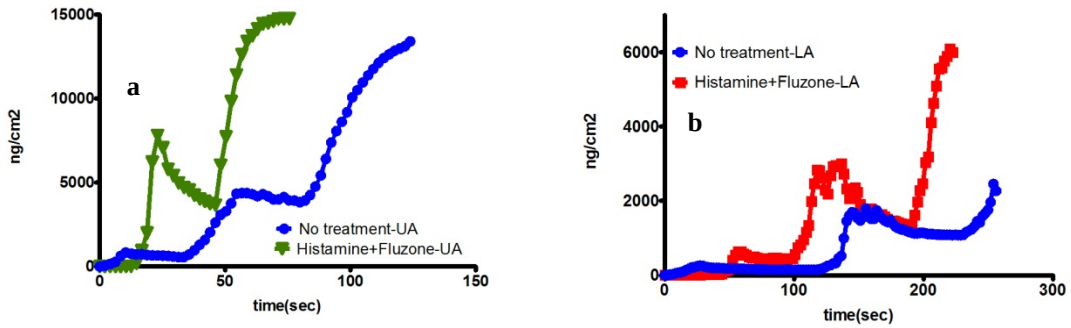

Figure A7: Aerosolized dosimetery on upper and lower airway with histamine plus Fluzone® antigen

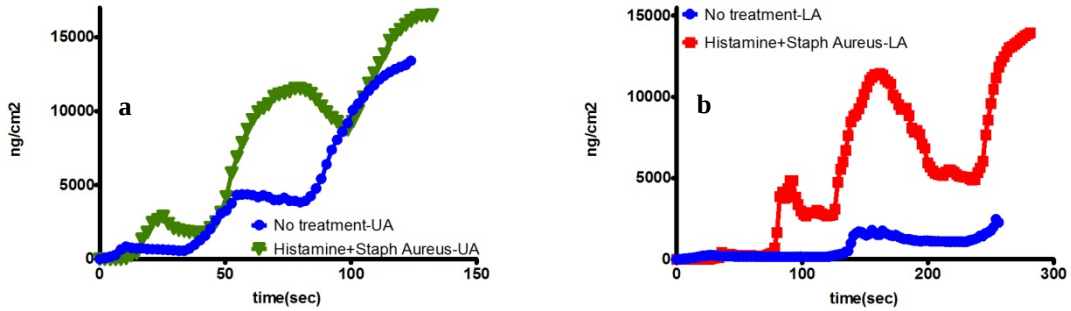

Figure A8: Aerosolized dosimetery on upper and lower airway with histamine plus staphylococcus Aureus bioparticles antigen

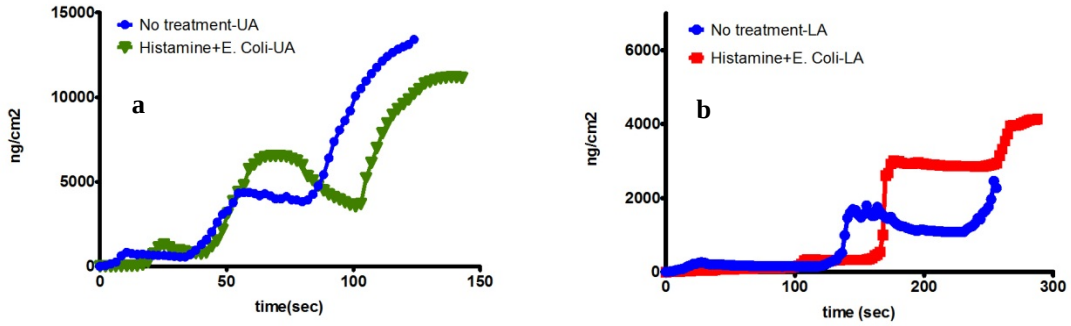

Figure A9: Aerosolized dosimetery on upper and lower airway with histamine plus e coli bioparticles antigen